hexagon:2611.01121v1

# HEEGAARD REALIZATIONS OF UNIFIED WRT INVARIANTS AND RADIAL COMPARISONS WITH $\widehat{Z}$: THE POINCARÉ SPHERE AND COMPLETION OBSTRUCTIONS

HAO-YU SUN

Abstract. We compare Heegaard realizations of the Witten–Reshetikhin–Turaev (WRT) invariant, Habiro's unified invariant, and homological-block $\widehat{Z}$ series, keeping their distinct coefficient and convergence domains. For the Poincaré sphere, a genus-two gluing adapted to an open-book page computes the canonical extended Reshetikhin–Turaev scalar at every root order $k \geq 2$. An explicit lift to a joint cyclotomic and power-series completion then recovers the oriented block, including its exceptional additive term. For Heegaard gluings with unimodular meridian-to-longitude block, finite Gram-matrix sewing and capping realize Habiro's known unified invariant in arbitrary genus. Composing this realization with Murakami's theorem gives a radial comparison on its stated class of negative-definite unimodular plumbings satisfying its leaf condition. Completion and nonuniqueness obstructions explain why root values alone do not determine a disk series; in particular, the matched-order Bailey polynomials for $\Sigma(2,3,7)$ do not form the required compatible cyclotomic sequence. A separate rank-one calculation identifies the refined scalar vacuum and its shifted refinement parameter.

## 1. Introduction

The Poincaré sphere provides a concrete benchmark for comparing Witten–Reshetikhin–Turaev (WRT) invariants computed by Heegaard gluing, unified closed invariants, and homological-block series. These objects have different targets. A finite-root Heegaard scalar lies in a root-dependent cyclotomic field. A unified closed invariant lies in the Habiro completion

$$\widehat{\mathbb{Z}[Q]}_{\mathrm{H}} = \varprojlim_{N} \mathbb{Z}[Q]/((Q)_N),$$

where $(Q)_N = \prod_{j=1}^{N}(1-Q^j)$. A *disk series* is considered on the open unit disk $|Q| < 1$; a radial endpoint is its limit along a radius approaching a root of unity, when that limit exists. After a branch of every fractional power is fixed, the Poincaré block studied below has the form

$$Q^{\Delta} f(Q), \qquad f(Q) \in \mathbb{Z}[[Q]],$$

on the corresponding finite cover of the punctured disk. Membership in $\mathbb{Z}[[Q]]$ is a formal condition; convergence on the disk is a separate analytic property of the block being used. The word "holomorphic" refers to the power-series factor after the displayed monomial is removed; regularity at $Q = 0$ is not asserted for the raw monomial-prefactored expression. A disk series itself is stronger data than all of its radial endpoints. Finally, an uncontracted boundary state has a different mathematical role and target from every one of these scalars. Every theorem below states its target explicitly.

The disk series belong to the homological-block program originating in the fivebrane construction of Gukov–Putrov–Vafa [13, Section 6.2] and the WRT reconstruction conjecture of Gukov–Pei–Putrov–Vafa [12, Conjecture 2.1]. Gukov–Manolescu's plumbing and knot-complement formulas [10, Sections 3.4, 4.6, and 5–7] provide the concrete blocks used here.

2020 *Mathematics Subject Classification.* Primary 57K31; Secondary 57K16, 13J10.
*Key words and phrases.* Heegaard splitting, unified WRT invariant, Habiro ring, Ohtsuki series, radial limit.

These disk objects are compared with Habiro's closed invariant through the specified normalization and radial limit, rather than by a map identifying their ambient completions.

The same marked Heegaard gluing is read at three successive levels. Capping the finite root data produces a cyclotomic scalar; compatible finite scalars then determine the closed Habiro element; and, only on the stated plumbing class, an independently defined disk series has a radial endpoint equal to the corresponding closed scalar. The uncapped boundary state is the input before these contractions, not a fourth name for one of the outputs. This is a distinction of mathematical type, not an assertion that the three constructions are interchangeable.

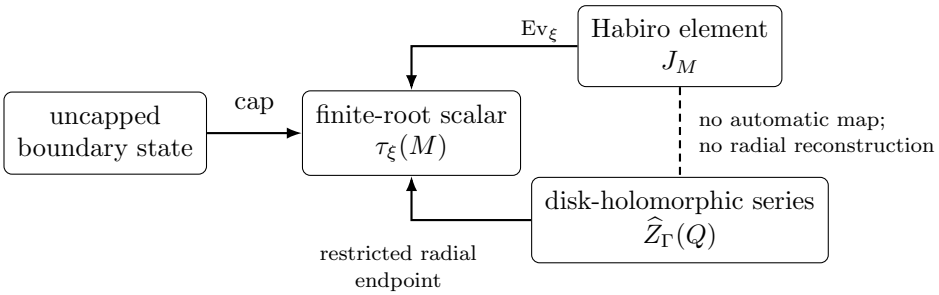



FIGURE 1. The three closed-output types and the uncapped input. A cap produces the finite scalar; a Habiro element specializes to it; and, on the stated plumbing class, an independently defined disk series has the prescribed radial endpoint. The dashed segment is not an arrow.

Let

$$M_\phi = H_g^- \cup_\phi H_g^+, \qquad \phi_* = \begin{pmatrix} A_\phi & B_\phi \\ C_\phi & D_\phi \end{pmatrix} \in \mathrm{Sp}_{2g}(\mathbb{Z})$$

in the meridian-column convention fixed in Section 2. The first headline result records a Heegaard realization of Habiro's closed invariant. Existence, uniqueness, and root specialization of that invariant are imported from Habiro; the contribution here is the presentation-level Gram/cap realization and its extension to arbitrary Heegaard genus.

Here an *integral homology sphere* (IHS) is a closed oriented three-manifold with the same integral homology as $S^3$. The finite-level construction uses a topological quantum field theory (TQFT), with its Reshetikhin–Turaev (RT) framing or weight extension. *Gram sewing* means contracting two pairing kernels with the inverse matrix of their finite-dimensional pairing. We call the construction *polarized* only to indicate that the state space and its algebraic dual are kept separate.

The proof of the closed construction follows four steps. First, the Heegaard matrix condition identifies the integral-homology-sphere locus. Second, finite polarized Gram sewing makes the capped root scalar independent of the chosen handlebody coordinates. Third, Habiro's established theorem identifies the compatible finite scalars with the unified invariant. Finally, successive polynomial lifts give the simultaneous root and Ohtsuki approximants, while the theorem's exclusions keep the result at the closed-scalar level.

**Theorem 1.1** (Heegaard cap and Gram realization)**.** *For every finite genus $g$ and every Heegaard word $\phi$ with $C_\phi \in \mathrm{GL}_g(\mathbb{Z})$, the closed manifold $M_\phi$ is an integral homology sphere. At every finite set of odd primes $p \geq 5$, the polarized finite TQFT kernels obey exact Gram sewing. After the two handlebody boundaries are capped, the resulting scalar is invariant under handlebody double-coset moves, complete fusion-coordinate changes, and Heegaard stabilization. Under Habiro's established existence, specialization, and uniqueness theorems, this scalar is the primitive odd-prime specialization of $J_{M_\phi}$. Thus the marked Heegaard presentation gives a Gram/cap realization of Habiro's known closed invariant. No clause constructs a non-IHS*

*block vector, an uncontracted all-root state, or a monomial-prefactored disk object on a fixed cover.*

*Proof.* The matrix condition first identifies the closed integral-homology-sphere locus. Finite polarized Gram sewing then makes the capped scalar independent of the allowed handlebody choices. The closed-cap comparisons in the companion paper on integral root fibers and closed factorizations [24] identify that scalar with the root specialization of Habiro's closed invariant. Each stage remains a closed scalar construction.

The theorem on Heegaard homological data in the companion paper on marked Heegaard boundary modules [25, Theorem 2.5] and its consequences here are Corollary 5.1 and Proposition 5.2. Finite-stage perfectness, Gram sewing, and capped invariance are Proposition 5.5 and Theorems 5.6 and 5.8. The exact closed-cap interfaces are Propositions 5.10 and 5.11. They apply here because unimodularity puts the closed manifold on the IHS locus and the comparison uses the raw empty-skein domain. The exclusions are proved by the scope statements following those results. □

Habiro's existence, uniqueness, injectivity, root specialization, and truncation properties are attributed inputs [14], not additional new clauses of Theorem 1.1. Their use in the present normalizations is recorded in Theorems 5.13 and 5.17, Corollary 5.14, and Lemma 5.16.

The exact Poincaré sphere supplies a convention-sensitive benchmark in which the finite and disk coordinates are linked by extra, manifold-specific data.

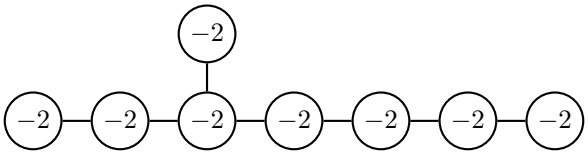



FIGURE 2. The negative-$E_8$ plumbing graph. Every vertex has weight $-2$, and the orientation convention used throughout is $P = \partial(-E_8) = \Sigma(2,3,5)$. The drawing adds no extra edge orientation, framing convention, or numerical invariant.

The benchmark is visible in the principal block $\widehat{Z}_0(P;Q) = Q^{-3/2}\big(2 - A(Q)\big)$, where the periodic series $A(Q)$ is defined in Section 3. This display is a guide to the closed Poincaré construction: the additive endpoint and the root/cover conventions are part of the theorem, not details that can be reconstructed from residue classes alone.

The Poincaré realization has four ingredients. The marked ribbon diagram fixes the orientation independently. The page-adapted genus-two gluing supplies the canonical finite RT scalar. The separate five-chain coordinates provide only the stated finite numerical checks. The joint-completion argument then identifies the distinguished Habiro component and its disk compression, including the exceptional additive endpoint.

**Theorem 1.2** (Poincaré gluing and joint Habiro/disk realization)**.** *Let $P = \partial(-E_8) = \Sigma(2,3,5)$ with the orientation and root branches of Equation (2.13). The page-adapted genus-two self-gluing decomposition and the canonical extended RT functor give $\tau_k(P)$ for every $k \geq 2$. The resulting Habiro component has the distinguished compatible Habiro/disk lift whose disk compression is*

$$\widehat{Z}_0(P;Q) = Q^{-3/2}\big(2 - A(Q)\big).$$

*The additive endpoint $2Q^{1/120}$ is part of the proof and cannot be recovered by reducing residue classes modulo 60 alone.*

*Proof.* The marked ribbon diagram fixes the oriented finite input, while the page-adapted self-gluing supplies the canonical all-level scalar. The joint completion argument connects the closed scalar to the displayed disk compression and retains the exceptional endpoint.

The oriented block and exceptional endpoint are Theorem 3.1 and Proposition 3.2. The marked ribbon diagram is established in Proposition 4.1 and Proposition 4.2; the independent page-adapted self-gluing is Proposition 4.3. The all-$k$ canonical TQFT/gluing equality is Theorem 4.7; it is not inferred from the finite validation table. The distinguished lift and its disk compression are Theorem 4.8. Their explicit composition is written out in the proof of Theorem 4.9. □

The separate Arthamonov–Shakirov five-chain/theta coordinates are not part of the headline theorem's conclusion. Their exact relative Maslov weight and finite residual test are recorded in Numerical Check 4.5; the missing all-level page-cap-to-theta and canonical-operator identifications are stated in Remarks 4.4 and 4.6.

The disk-side comparison is the attributed composition of the Heegaard realization with Murakami's radial theorem in exactly its stated plumbing range. After matching the WRT, plumbing-block, and radial conventions, we apply that theorem on the stated negative-definite plumbing class and compose the endpoint identity with arbitrary-genus Habiro descent. No general radial comparison outside this class is asserted. Write $\zeta_n = e^{2\pi i/n}$, let $\mathrm{Ev}_\xi$ denote evaluation of a Habiro element at $\xi$, and let $\mathrm{Rad}_{Q\to\zeta_k}$ denote the limit along $Q = \zeta_k e^{-t}$, $t \downarrow 0$, with lifted logarithm $2\pi i/k - t$.

**Theorem 1.3** (Restricted radial comparison)**.** *Let $\Gamma$ be a negative-definite unimodular plumbing tree such that*

$$|\overline{v}| + 2 - \deg(v) > 0 \qquad \text{for every } v \in V_{\geq 3}.$$

*Here $V_{\geq 3}$ consists of vertices of degree at least three, and $\overline{v}$ is the set of leaves adjacent to $v$. For every orientation-preserving identification $M_\phi \cong M(\Gamma)$ and every $k \geq 3$,*

$$\mathrm{Rad}_{Q\to\zeta_k} \widehat{Z}_\Gamma(Q) = 2(\zeta_{2k} - \zeta_{2k}^{-1})\,\mathrm{Ev}_{\zeta_k} J_{M_\phi}.$$

*At odd primes this Habiro evaluation is the normalized capped Heegaard scalar in every genus.*

*Proof.* Match the finite WRT, plumbing-block, and radial normalizations first. The restricted plumbing theorem supplies the radial endpoint identity, and Habiro descent identifies its finite side with the closed Heegaard scalar. The plumbing and unimodularity hypotheses therefore remain visible at the point where the comparison is used.

The exact source theorem and both normalization bridges are Lemmas 6.1 and 6.2 and Theorem 6.3. Their composition with Theorem 5.13 is Theorem 6.5. □

The comparison is sharp in two different senses. The raw matched-order Bailey polynomials for $\Sigma(2,3,7)$ do not form a Habiro-projective tower (Theorem 6.10); and root endpoints do not determine a disk series (Proposition 6.11 and Corollary 6.12). The only positive refined statement in this paper is the scalar identity of Theorem 7.1 and the formal algebra of Proposition 7.3. The refined state-space rank and the arbitrary-genus refined modular functor are not claimed.

**Relation to previous work.** The geometric and finite-TQFT inputs are the marked Poincaré diagram, open-book, page-adapted self-gluing, and five-chain results of [17, 9, 4, 23, 19, 3], and the finite TQFT gluing and capped-scalar formalism of [5, 8, 2]. The completion and q-series comparison uses Habiro's unified invariant and its injectivity and specialization theorems [14], the oriented plumbing blocks of [10], the Poincaré strange identity of [16], the radial theorem of [22], the Bailey identity of [20]. Murakami's later theorem [21, Theorem 1.2] treats the weighted radial combination for general negative-definite plumbing trees, without asserting all individual block limits. Section 6 explains this broader result; the comparison proved here retains the earlier unimodular, leaf-restricted hypotheses. The homology and obstruction results come from the marked boundary-module construction [25]; the closed-cap comparisons come from the integral-root-fiber construction [24]. This paper does not reprove these inputs. Its

contribution is to organize the finite polarized Gram/cap calculation, prove the Poincaré joint completion and its compression by the Chinese remainder theorem and cyclotomic divisibility, pass from arbitrary-genus capped scalars to one Habiro invariant, prove the two convention bridges, compose them with the restricted radial theorem, and isolate the Bailey, completion-map, and refined scope boundaries. The finite coordinate calculations remain checks on the displayed formulas, and no claim of novelty is inferred merely from this composition.

## 2. The Heegaard problem and fixed conventions

The closed invariant begins with a Heegaard gluing and a finite-root state space. This section fixes the orientation, marking, symplectic convention, and normalization denominator before the paper passes to Habiro or disk coordinates.

2.1. **The problem.** Let $H_g$ be an oriented genus-$g$ handlebody and let $\Sigma_g = \partial H_g$. Write $\mathrm{MCG}(\Sigma_g)$ for the orientation-preserving mapping class group. With the incoming handlebody orientation reversed, as in $H_g^- \cup_\phi H_g^+$, we abbreviate the Heegaard gluing by

$$M_\phi = H_g \cup_\phi H_g, \qquad \phi \in \mathrm{MCG}(\Sigma_g). \tag{2.1}$$

At a root of unity, a modular tensor category assigns a state space to $\Sigma_g$, a handlebody vector to $H_g$, and a projective mapping-class operator to $\phi$. After the extended-mapping-class or framing lift is fixed, the closed invariant is a calibrated matrix element

$$\tau_k(M_\phi) = \frac{\langle v_{H_g}, \rho_k(\phi) v_{H_g}\rangle}{\langle v_{H_g}, \rho_k(\phi_{S^3}) v_{H_g}\rangle}. \tag{2.2}$$

Here $v_{H_g}$ is the handlebody state, $\rho_k$ is the lifted mapping-class action, and $\phi_{S^3}$ is a gluing giving $S^3$ in the same normalization. The denominator is part of the convention: a bare vacuum matrix element is not automatically normalized by $\tau_k(S^3) = 1$.

The harder question is not the finite TQFT statement. It is to determine when closed Heegaard data have a cyclotomic lift and when that lift can be compared with an independently defined monomial-prefactored series on a fixed cover of the punctured disk. The two completions are not identified. Any comparison must retain the information discarded by the homological action and recover the correct framing and orientation [13, 12].

It is useful to separate four layers from the outset.

(1) The *marked geometry* consists of two cut systems, their embeddings and surface framings, and a representative of the relevant handlebody double coset.
(2) The *homological data* consist of the symplectic action and the finite linking module.
(3) The *nonabelian operator* is assembled from twists and recouplings in a trivalent-spine basis; in genus two its local kernels are quantum $6j$ symbols.
(4) The *completion and cap* first produce a closed cyclotomic scalar. Disk data enter only through a separate comparison theorem.

Agreement at only one layer never substitutes for the remaining layers. In particular, a balanced group presentation is not a marked Heegaard diagram, a symplectic matrix is not a mapping class, and all root-of-unity values do not by themselves determine such a fixed-cover disk function.

The marked gluing and spine determine the finite-root calculation; the homological data identify the integral-homology-sphere locus used for the Habiro lift considered here. The later plumbing and radial hypotheses then compare that scalar with an independently defined disk series. Thus each transition uses information that the preceding output alone does not retain.

2.2. **Markings and the double-coset ambiguity.** Let $\mathcal{H}_g \subset \mathrm{MCG}(\Sigma_g)$ be the handlebody group, consisting of mapping classes that extend over $H_g$. Changing either handlebody marking changes a representative $\phi$ without changing the splitting, so the geometric gluing datum naturally lives in

$$\mathcal{H}_g \backslash \mathrm{MCG}(\Sigma_g)/\mathcal{H}_g. \tag{2.3}$$

There is therefore no canonical word in Dehn twists. A usable word requires a chosen surface marking, a chosen trivalent spine, and a convention for composition. If $G$ changes the marking, then the coordinate operator is $\rho(G)^{-1}\rho(\phi)\rho(G)$, together with the corresponding projective or Maslov correction. Conjugation by a mapping class extending over a cap can leave the vacuum amplitude unchanged even though the displayed word changes.

**Definition 2.1** (marked Heegaard input)**.** A marked input for a computational theorem consists of:

(1) ordered, oriented cut systems on the two sides of $\Sigma_g$;
(2) enough cyclic-order and intersection-sign data to reconstruct their embeddings;
(3) the surface-framing convention;
(4) a trivalent-spine marking of the first handlebody;
(5) an explicit curve-level mapping-class factorization or an equivalent marked diagram with explicit reconstruction data.

Free-group words obtained after retracting curves into a handlebody are only shadows of this input.

2.3. **Symplectic convention and the linking form.** Choose a symplectic basis

$$(a_1, \dots, a_g, b_1, \dots, b_g) \tag{2.4}$$

in which the $a_i$ bound disks in the first handlebody. We write the homological action in blocks as

$$\phi_* = \begin{pmatrix} A & B \\ C & D \end{pmatrix} \in \mathrm{Sp}(2g, \mathbb{Z}). \tag{2.5}$$

The companion boundary-object paper proves the direct column-relation presentation in its theorem on the homological data of the Heegaard splitting [25, Theorem 2.5]:

$$G_{\mathrm{col}} = \mathbb{Z}^g / C\mathbb{Z}^g.$$

For the quadratic coordinates used below, that theorem passes to the canonically isomorphic row-relation model

$$H_1(M_\phi; \mathbb{Z}) \cong G_{\mathrm{row}} := \mathbb{Z}^g / C^T\mathbb{Z}^g, \qquad Q_\phi = C^{-1}D \pmod{\mathbb{Z}}, \tag{2.6}$$

whenever $C$ is nonsingular. The coordinate change is

$$\overline{D} : G_{\mathrm{row}} \xrightarrow{\sim} G_{\mathrm{col}}, \qquad [u] \longmapsto [Du],$$

with inverse $[x] \mapsto [A^T x]$. Indeed, $DC^T = CD^T$, $A^TC = C^TA$, $A^TD - C^TB = I$, and $DA^T - CB^T = I$. The symplectic relation $CD^T = DC^T$ implies

$$(C^{-1}D)^T = D^TC^{-T} = C^{-1}D, \tag{2.7}$$

so $Q_\phi$ is symmetric, and $CQ_\phi = D$ shows directly that it descends on $G_{\mathrm{row}}$.

In the direct column model the same linking form is represented instead by $AC^{-1}$. Thus a formula written in row coordinates must be transported by $\overline{D}$ before it is used on $\mathrm{coker}(C)$. The matrices $C^{-1}D$ and $DC^{-1}$ cannot be interchanged in general. Diagonal examples cannot detect the difference, which is why non-diagonal examples are essential convention tests.

2.4. **Root, level, and color conventions.** The global coefficient dictionary is

$$Q = Q_{\mathrm{Habiro}} = Q_{\widehat{Z}} = A^4, \qquad q_{\mathrm{Cost}} = A^2.$$

Here $A$ is the Kauffman-bracket parameter and $q_{\mathrm{Cost}}$ is the quantum parameter in the convention of Costantino [7]. This is an equality of coordinate variables, not an identification of the Habiro and disk completions. We distinguish $Q$ from all root-of-unity specializations. For the $SU(2)$ category, set

$$k \geq 2, \qquad \ell = k - 2, \qquad \zeta_k = e^{2\pi i/k}. \tag{2.8}$$

The integer color $j \in \{0, \dots, \ell\}$ denotes spin $j/2$. At generic $Q$ we use the symmetric quantum integer

$$[n]_Q = \frac{Q^{n/2} - Q^{-n/2}}{Q^{1/2} - Q^{-1/2}}, \qquad [n]_Q! = \prod_{r=1}^{n} [r]_Q. \tag{2.9}$$

At a root, branch choices involving $Q^{1/2}$ are fixed by $\zeta_k^{1/2} = e^{\pi i/k}$. A formula with category level $\ell$ must not silently replace the root order $k = \ell + 2$ by $\ell$.

We normalize the WRT invariant by

$$\tau_k(S^3) = 1. \tag{2.10}$$

This does not normalize the disk block to one. In the reduced convention used below,

$$\widehat{Z}_0(S^3; Q) = 2\big(Q^{1/2} - Q^{-1/2}\big). \tag{2.11}$$

The Weyl-denominator factor in (2.11) is precisely what relates the radial limit of a block to an $S^3$-normalized WRT invariant.

2.5. **The orientation fixed for the Poincaré sphere.** Write

$$P = \partial(-E_8) = \Sigma(2, 3, 5). \tag{2.12}$$

Our orientation dictionary is

$$\boxed{P = S^3_{-1}(\overline{T}_{2,3}) = -S^3_{+1}(T_{2,3}),} \tag{2.13}$$

where $T_{2,3}$ is the right-handed trefoil and $\overline{T}_{2,3}$ is its mirror. Thus a $+1$ right-handed-trefoil presentation targets $-P$, not $P$. Orientation reversal complex conjugates the finite WRT invariant and changes the disk block nontrivially; it is not an overall monomial convention.

2.6. **Finite reconstruction and checking data.**

**Definition 2.2** (Finite verification data)**.** Finite verification data for a stated claim specify the combinatorial or algebraic input, the conventions, and a calculation that a reader can check. For a marked Heegaard diagram, the data give the signed cyclic intersection orders and surface framings needed to reconstruct the diagram. For an exact matrix identity, they give the matrices and the identity to be checked. A numerical check also records its tested parameters and precision; such data support only the stated finite check.

For the marked Poincaré diagram, the finite input consists of signed cyclic intersection orders and the oriented surface convention. Pairing successive half-edges reconstructs the ribbon surface; its face cycles determine the genus, and the signed crossings determine the intersection matrices (Proposition 4.1 and Proposition 4.2). The recorded attaching relators give a separate fundamental-group check. For the page-adapted construction, the monodromy, the eight ordered slides, and the self-gluing map are the geometric input (Equations (4.17) and (4.18)); the extended RT gluing axiom then computes the canonical scalar. The separate five-chain calculations test the displayed word, phase, and normalization at the stated levels; their finite agreement does not supply the all-level gluing proof.

Numerical agreement at finitely many levels can detect a wrong word, phase, or normalization, but it does not establish an all-level identity. Conversely, an all-level topological proof still needs explicit convention checks before it identifies a particular displayed matrix product. The statements below distinguish exact reconstruction, numerical evidence, and unresolved identifications.

2.7. **Scope of the closed construction.** The trivalent basis, local $6j$ calculus, and homological data do not by themselves define a generic boundary invariant. The positive theorem in this paper contracts both handlebody boundaries at each finite root and only then performs Habiro descent on the integral-homology-sphere locus. The Poincaré case has extra manifold-specific joint data; the radial comparison has the separate plumbing hypotheses stated in Theorem 1.3.

## 3. The corrected Poincaré target

The Poincaré sphere is the convention-sensitive test case: it exposes the orientation, fractional-power, and exceptional-endpoint data that a general closed-scalar theorem can hide. This section defines the corrected block before constructing the marked genus-two gluing.

3.1. **The false theta series and the oriented block.** Define the periodic function $\chi_{60} : \mathbb{Z} \to \{-1, 0, 1\}$ by

$$\chi_{60}(m) = \begin{cases} +1, & m \equiv 1, 11, 19, 29 \pmod{60}, \\ -1, & m \equiv 31, 41, 49, 59 \pmod{60}, \\ 0, & \text{otherwise.} \end{cases} \tag{3.1}$$

Set

$$A(Q) = \sum_{m \geq 1} \chi_{60}(m) Q^{(m^2-1)/120}. \tag{3.2}$$

This is a false theta series: the periodic coefficient is odd under $m \mapsto -m$, and the sum retains the positive integers rather than summing symmetrically over $\mathbb{Z}$. Every nonzero residue in (3.1) has square congruent to one modulo 120, so $A(Q) \in \mathbb{Z}[[Q]]$. Its beginning is

$$A(Q) = 1 + Q + Q^3 + Q^7 - Q^8 - Q^{14} - Q^{20} - Q^{29} + Q^{31} + \cdots . \tag{3.3}$$

The residue calculation is correct, but $A(Q)$ alone is not the homological block of $P$.

Let

$$\chi_0(Q) = \sum_{n \geq 0} \frac{Q^n}{(Q^{n+1}; Q)_n}, \qquad (a; Q)_n = \prod_{j=0}^{n-1} (1 - aQ^j). \tag{3.4}$$

The following theorem is an imported block calculation: in the fixed orientation it is the Poincaré example and Brieskorn plumbing formula of [10, Section 3.4, equations (26)–(28), and Proposition 4.8], with the radial normalization also agreeing with [18]. It is used as a named input and is not rederived here.

Gukov–Manolescu attribute the resurgence calculation of this block to Gukov–Mariño–Putrov [11, Section 3.4]. The negative-plumbing formula below uses the normalization printed by Gukov–Manolescu, including its exceptional additive term.

**Theorem 3.1** (oriented Poincaré blocks)**.** *In the orientation convention $P = \partial(-E_8) = \Sigma(2, 3, 5)$ of (2.13),*

$$\widehat{Z}_0(P; Q) = Q^{-3/2}\big(2 - A(Q)\big), \tag{3.5}$$

$$\widehat{Z}_0(-P; Q) = Q^{3/2}\big(2 - \chi_0(Q)\big). \tag{3.6}$$

*In particular, the two orientations are not related by changing only an overall sign or monomial power.*

The opposite-orientation formula is recorded in [10, Section 3.4, following Theorem 3.9]; it is not obtained from the first formula by a monomial change.

This example also belongs to the false-/mock-theta picture of orientation reversal studied in [6, Section 7], where a general relation is proposed and specific examples are analyzed.
The endpoint correction and its role. The displayed pair of formulas separates the orientation-sensitive output from the residue calculation that helps describe it. The series $A(Q)$ records the periodic contribution, but the next step must still account for the exceptional lower endpoint in the oriented plumbing reduction. The endpoint proposition identifies that missing contribution and combines its fractional power with the residue series; it is therefore a correction to the block formula, not a renormalization of $A(Q)$ and not a new radial normalization.

After removing the leading $Q^{-3/2}$ from (3.5),

$$Q^{3/2}\widehat{Z}_0(P;Q) = 1 - Q - Q^3 - Q^7 + Q^8 + Q^{14} + Q^{20} + Q^{29} - Q^{31} - \cdots . \tag{3.7}$$

3.2. **The exceptional endpoint.** For pairwise coprime $(b_1, b_2, b_3)$ put $p = b_1b_2b_3$ and

$$\alpha_1 = p - b_1b_2 - b_1b_3 - b_2b_3, \tag{3.8}$$

$$\alpha_2 = p + b_1b_2 - b_1b_3 - b_2b_3, \tag{3.9}$$

$$\alpha_3 = p - b_1b_2 + b_1b_3 - b_2b_3, \tag{3.10}$$

$$\alpha_4 = p + b_1b_2 + b_1b_3 - b_2b_3. \tag{3.11}$$

For $(2, 3, 5)$ these are

$$(\alpha_1, \alpha_2, \alpha_3, \alpha_4) = (-1, 11, 19, 31). \tag{3.12}$$

The negative value $\alpha_1 = -1$ changes a lower summation endpoint in the Brieskorn reduction. In the oriented Brieskorn formula of [10, Proposition 4.8, equation (56)], this produces a term that is invisible after reducing all indices modulo 60.

**Proposition 3.2** (exceptional endpoint)**.** *For the* $(2, 3, 5)$ *negative-plumbing calculation,*

$$C_{235} = 2Q^{1/120}, \qquad \Delta_{235} = -\frac{181}{120}, \qquad \Phi_{235}(Q) = Q^{1/120}A(Q). \tag{3.13}$$

*Consequently*

$$Q^{\Delta_{235}}\big(C_{235} - \Phi_{235}(Q)\big) = Q^{-3/2}\big(2 - A(Q)\big). \tag{3.14}$$

*Proof.* The endpoint at $(2, 3, 5)$ must be retained before the residue classes are reduced. The following calculation shows the additive contribution that would otherwise be lost.

Specializing the endpoint term of [10, Proposition 4.8 and the end of its proof] at $(2, 3, 5)$ gives $2Q^{1/120}$. Factoring the common $Q^{1/120}$ from the endpoint and false theta gives

$$-\frac{181}{120} + \frac{1}{120} = -\frac{3}{2}, \tag{3.15}$$

which proves (3.14). □

This endpoint is a diagnostic for every proposed direct recoupling derivation. A calculation that retains only the eight nonzero residue classes modulo 60 can reproduce $A(Q)$ while still missing the block.

3.3. **Finite normalization and radial limits.** Let $\tau_k$ be normalized by $\tau_k(S^3) = 1$, and use the radial branch $\zeta_k^{1/2} = e^{\pi i/k}$. The Lawrence–Zagier radial theorem [18] in the present convention is

$$\boxed{\operatorname*{rad\,lim}_{Q\to\zeta_k} \widehat{Z}_0(P;Q) = 2\big(\zeta_k^{1/2} - \zeta_k^{-1/2}\big)\tau_k(P).} \tag{3.16}$$

Equivalently, using (2.11),

$$\lim_{Q\to\zeta_k}{}^{\mathrm{rad}}\ \frac{\widehat{Z}_0(P;Q)}{\widehat{Z}_0(S^3;Q)}=\tau_k(P). \tag{3.17}$$

Thus an $S^3$-normalized vacuum amplitude is compared with a ratio of blocks, not directly with $A(Q)$ or with a block normalized to have constant term one.

3.4. **Why radial data do not select a disk series.** The infinite Euler product

$$(Q;Q)_\infty=\prod_{n\geq 1}(1-Q^n) \tag{3.18}$$

is holomorphic for $|Q|<1$ and has radial value zero at every root of unity. Hence adding a polynomial multiple of $(Q;Q)_\infty$ preserves all radial values. Root data alone therefore do not distinguish arbitrary disk functions.

*Remark* 3.3 (the rank-one shortcut is circular). Declaring the allowed functions to be the span of a proposed answer and then assuming that the unknown Heegaard extraction belongs to that span does not prove the membership assumption. A single abelian block label is a label-counting statement; it does not make the analytic target space one-dimensional.

The missing structure can be a generic-$Q$ construction, a growth theorem, or a distinguished lift compatible with the cyclotomic and disk data. For $P$, the last option is available explicitly.

3.5. **The Poincaré Habiro bridge.** Following Habiro's unified Poincaré formula [14], define

$$J_P(Q)=\frac{1}{1-Q}\sum_{m\geq 1}Q^{m-1}(Q^m;Q)_m. \tag{3.19}$$

At a root of unity different from one, the sum truncates and evaluates the unified WRT invariant [14]. The Poincaré strange identity [16, 14] gives the coefficientwise disk series

$$A(Q)=\sum_{n\geq 0}Q^n(Q^n;Q)_n. \tag{3.20}$$

Separating the $n=0$ term yields the exact bridge

$$A(Q)=1+Q(1-Q)J_P(Q), \tag{3.21}$$

where the right side is understood through the distinguished lift compatible with the cyclotomic and disk data, not as an assertion that every Habiro element has a disk expansion. Substitution into the oriented block formula of [10, Section 3.4, equation (26)] gives

$$\widehat{Z}_0(P;Q)=Q^{-3/2}\big(1-Q(1-Q)J_P(Q)\big). \tag{3.22}$$

The two realizations carry different information. The cyclotomic component is determined by root evaluations; the coefficientwise $\mathbb{Z}[[Q]]$ component is additional data. Section 4 constructs the joint element used in (3.21).

3.6. **From the block formula to the marked gluing.** The block computation provides the following data:

(1) the residue function (3.1) and integrality of its exponents;
(2) the oriented blocks (3.5) and (3.6);
(3) the endpoint formula (3.14);
(4) the radial normalization (3.16);
(5) the Poincaré-specific joint identity (3.21).

What remains at this stage is to derive the finite invariant from a fully marked and normalized genus-two operator, and then to show that the distinguished compatible lift is the one attached to that finite invariant. The next section supplies both statements for $P$ without claiming a universal block-extraction theorem.

## 4. Genus-two gluing and a joint lift for the Poincaré sphere

The page-adapted genus-two self-gluing identifies the closed manifold before the finite TQFT gluing axiom computes its invariant. The signed ribbon diagram independently identifies the same oriented manifold. The five-chain/theta coordinates then test the finite scalar and phase; their role remains distinct from the all-level gluing proof.

4.1. **From the gluing to the joint lift.** The page-adapted gluing gives the Poincaré-specific chain:

$$\begin{aligned}\text{page-adapted genus-two self-gluing} &\longrightarrow \text{canonical extended RT scalar}\\ &\longrightarrow \text{distinguished joint Habiro/disk lift.}\end{aligned} \tag{4.1}$$

Every arrow has a geometric or algebraic proof. The signed ribbon diagram in the next subsection independently gives a genus-two diagram for the same oriented manifold. The Arthamonov–Shakirov five-chain/theta coordinates later in the section provide independent finite checks. No explicit marking change from either the ribbon code or the page-adapted self-gluing cap to that theta cap is asserted. Symbolic calculations supply discriminating falsification tests; they are not used to replace the all-level TQFT argument.

4.2. **The marked ribbon diagram.** Take ordered, oriented lower curves $\ell_1, \ell_2$ and upper curves $u_1, u_2$. The cyclic presentation is the Poincaré Heegaard code recorded by Kashaev–Virelizier [17]; its based intersection orders are

$$\ell_1 = (1,2,3,4,5,6,7), \qquad \ell_2 = (a,b,c,d,e), \tag{4.2}$$

$$u_1 = (1,2,3,4,a,6,c), \qquad u_2 = (b,7,d,e,5). \tag{4.3}$$

The positive intersections are

$$\{1,2,3,4,d,e\}, \tag{4.4}$$

and the negative intersections are

$$\{5,6,7,a,b,c\}. \tag{4.5}$$

Together with the oriented surface convention, these lists determine the local ribbon rotation at every crossing. Pairing successive half-edges along each oriented curve gives a finite combinatorial map.

**Proposition 4.1** (ribbon reconstruction)**.** *The signed code* (4.2)–(4.3) *reconstructs a connected oriented surface with*

$$V = 12, \qquad E = 24, \qquad F = 10, \qquad \chi = -2, \qquad g = 2. \tag{4.6}$$

*Its face lengths are six* 4*-cycles and four* 6*-cycles. With upper curves as rows and lower curves as columns, its geometric and algebraic intersection matrices are*

$$G = \begin{pmatrix} 5 & 2 \\ 2 & 3 \end{pmatrix}, \qquad I = \begin{pmatrix} 3 & -2 \\ -2 & 1 \end{pmatrix}. \tag{4.7}$$

*Moreover,*

$$\det I = -1, \qquad \mathrm{SNF}(I) = I_2. \tag{4.8}$$

*Here* SNF *denotes Smith normal form, with positive diagonal entries.*

*Proof.* The cyclic code determines the surface through its face cycles and the intersection matrices through its crossings.

The vertex rotation and edge involution are read directly from the signed cyclic lists. Their product has the stated ten face cycles, giving $12 - 24 + 10 = -2$. Summing absolute and signed crossings for each upper/lower pair gives $G$ and $I$. The determinant and Smith form are immediate exact integer calculations. □

The independent planar description of Guadagnini–Mathieu–Thuillier [9] reads the attaching relators

$$r_1 = x^{-4}yxy, \qquad r_2 = y^{-2}xyx. \tag{4.9}$$

Their exponent matrix is

$$E = \begin{pmatrix} -3 & 2 \\ 2 & -1 \end{pmatrix} = -I, \tag{4.10}$$

which independently checks all four signed intersections. If

$$s_1 = (xy)^2x^{-5}, \qquad s_2 = (xy)^2y^{-3}, \tag{4.11}$$

then free reduction gives

$$r_1 = x^{-5}s_1x^5, \qquad r_2 = y^{-2}s_2y^2. \tag{4.12}$$

Thus the normal closure gives the binary-triangle presentation

$$\langle x, y \mid x^5 = y^3 = (xy)^2 \rangle. \tag{4.13}$$

For example, over $\mathbb{F}_5$ the matrices

$$X = \begin{pmatrix} 0 & 1 \\ 4 & 3 \end{pmatrix}, \qquad Y = \begin{pmatrix} 0 & 4 \\ 1 & 1 \end{pmatrix} \tag{4.14}$$

satisfy

$$X^5 = Y^3 = (XY)^2 = -I, \tag{4.15}$$

and generate all 120 elements of $SL(2, \mathbb{F}_5)$. This is an exact finite witness for the nontrivial binary-icosahedral quotient, while the primary marked-diagram identification supplies the topological identification.

**Proposition 4.2** (A marked Poincaré diagram)**.** *The signed code (4.2)–(4.3), with its surface framings, is a marked genus-two Heegaard diagram for the Poincaré homology sphere. Its first homology is trivial and its fundamental group is binary icosahedral.*

*Proof.* Proposition 4.1 proves that the code is a genus-two diagram and that its attaching matrix is unimodular. Equations (4.9)–(4.13) identify its fundamental group. The independent diagram descriptions in [17, 9] identify it as Poincaré's. The orientation used below is fixed separately by the positive open-book monodromy and its negative-trefoil surgery dual, not by the unoriented group presentation. □

4.3. **The page-adapted self-gluing and a five-chain coordinate candidate.** Let $S_{1,1}$ be a once-punctured torus with dual curves $a, b$. The Poincaré open book and its surgery orientation are those of [4]; in the chosen orientation its monodromy is

$$h = (T_aT_b)^5. \tag{4.16}$$

Here $T_a, T_b$ are positive Dehn twists. Doubling the page gives a genus-two Heegaard surface and an adapted gluing representative [23]. We use the self-gluing handlebody $H_{\mathrm{sg}}$ of Lipshitz–Ozsváth–Thurston [19, Section 9.5, Definition 9.12 and Figures 44–45]. In their genus-two split

pointed-matched-circle marking it is obtained from the split handlebody by the eight ordered slides

$$\begin{aligned} &5 \text{ over } 4, \quad 2 \text{ over } 1, \quad 3 \text{ over } 2, \quad 4 \text{ over } 3, \\ &2 \text{ over } 1, \quad 6 \text{ over } 5, \quad 7 \text{ over } 6, \quad 2 \text{ over } 3. \end{aligned} \tag{4.17}$$

Denote the two page arc slides called $A, B$ in that source by $\mathsf{A}_{\mathrm{pg}}, \mathsf{B}_{\mathrm{pg}}$ here, to avoid collision with the bracket coordinate and the five-chain generators. Write $Y_\Psi$ for the mapping cylinder of a page-induced gluing map $\Psi$.

**Proposition 4.3** (The page-adapted Poincaré self-gluing)**.** *With the positive-open-book orientation,*

$$P = -H_{\mathrm{sg}} \cup Y_{\Psi_P} \cup H_{\mathrm{sg}}, \qquad \Psi_P = (\mathsf{A}_{\mathrm{pg}}\mathsf{B}_{\mathrm{pg}})^5. \tag{4.18}$$

*Proof.* The doubled-page construction gives the genus-two Heegaard surface [23]. Lipshitz–Ozsváth–Thurston define $H_{\mathrm{sg}}$, give the eight slides in (4.17), extend the two page twists to the genus-two mapping cylinders, and identify the capped cylinder $-H_{\mathrm{sg}} \cup Y_{(AB)^5} \cup H_{\mathrm{sg}}$ with the Poincaré sphere [19, Section 9.5]. The positive monodromy and negative-trefoil surgery dual fix the orientation $P = \partial(-E_8)$ [4]. □

There is also a useful five-chain coordinate candidate. In the Arthamonov–Shakirov marking [3], choose

$$a = B_1, \qquad b = T_{A_2}(B_2), \qquad T_b = A_2 B_2 A_2^{-1}. \tag{4.19}$$

These are dual curves on the fixed closed surface. Their conjugation can be checked in the hyperelliptic braid model. Put

$$G_0 = A_2^{-1} B_1^{-1} A_1^{-1} B_2, \qquad g = G_0^{-1} = B_2^{-1} A_1 B_1 A_2. \tag{4.20}$$

Under the map from the six-strand braid group $B_6$ to the genus-two five-chain, $g = \sigma_4^{-1}\sigma_1\sigma_2\sigma_3$, and the braid relations give

$$g\sigma_1 g^{-1} = \sigma_2, \qquad g\sigma_2 g^{-1} = \sigma_3\sigma_4\sigma_3^{-1}. \tag{4.21}$$

The faithful Artin action on the free group $F_6$ verifies these as identities of curves. Thus the corresponding exact five-chain representative of the page mapping class is

$$\boxed{M_P^{\mathrm{five}} = G_0^{-1}(A_1B_1)^5 G_0 = (B_1A_2B_2A_2^{-1})^5.} \tag{4.22}$$

Products are read with the rightmost factor acting first. The positive $(3,5)$ braid lift is surgery-dual to the negative trefoil in the orientation convention of [4]. This fixes the intended orientation of the coordinate candidate; it does not identify its theta cap with $H_{\mathrm{sg}}$.

As a necessary homological check, in the five-chain marking

$$(M_P^{\mathrm{five}})_* = \begin{pmatrix} 0 & 1 & 1 & 1 \\ -1 & 2 & 1 & 1 \\ -1 & 0 & 1 & 0 \\ 1 & -1 & -1 & 0 \end{pmatrix}, \qquad C = \begin{pmatrix} -1 & 0 \\ 1 & -1 \end{pmatrix}. \tag{4.23}$$

Thus $\det C = 1$. The open book and curve identities, not this determinant, identify the mapping class. The determinant does not supply the missing change of handlebody marking.

*Remark* 4.4 (No page-cap-to-theta identification). The source for Proposition 4.3 supplies the adapted self-gluing handlebody and its eight slides from the split handlebody, but it does not translate those slides and the two page cylinders into the fixed Arthamonov–Shakirov theta marking. Consequently we do not claim that

$$\frac{\langle 0|\rho_k^{\mathrm{five}}(M_P^{\mathrm{five}})|0\rangle}{\langle 0|\rho_k^{\mathrm{five}}(I)|0\rangle} = \tau_k(P) \tag{4.24}$$

holds for every $k$, where $\rho_k^{\mathrm{five}}$ denotes the five-chain extended operator defined below. The theta-vacuum ratio, the five-chain Maslov lift, and the printed matrices below are finite coordinate validation only. The all-level theorem uses (4.18) and its canonical handlebody vectors instead.

4.4. **The printed quantum-6j coordinate candidate.** The theta basis is indexed by admissible colorings of the graph with two vertices joined by three edges. In this subsection, the superscript AS refers to the Arthamonov–Shakirov coordinates. Fix $k \geq 2$, put $\ell = k-2$ and $Q = e^{2\pi i/k}$, and define

$$S_{00} = \sqrt{\frac{2}{k}} \sin\frac{\pi}{k}, \qquad \xi_k = \exp\left(\frac{3\pi i(k-2)}{4k}\right), \qquad d_j = \frac{\sin((j+1)\pi/k)}{\sin(\pi/k)}. \tag{4.25}$$

An admissible triple has $0 \leq j_i \leq \ell$, satisfies the triangle inequalities, and has even sum at most $2\ell$ [3, arXiv v3, Section 1, equation (6)]. On the admissible theta basis, let

$$G_{(j_1,j_2,j_3)} = \frac{1}{d_{j_1} d_{j_2} d_{j_3}} \tag{4.26}$$

be the diagonal basis metric. Let $B_n^{\mathrm{AS}}$ be the printed finite genus-two matrix built from squared, level-truncated quantum $6j$ symbols, with the $B_1, B_2$ entries given by the formulas in [3]. Define

$$B_n^U = S_{00} B_n^{\mathrm{AS}}, \qquad B_n^{\mathrm{coh}} = \xi_k B_n^U. \tag{4.27}$$

The $A$ twists act by

$$A_n |j_1, j_2, j_3\rangle = Q^{j_n(j_n+2)/4} |j_1, j_2, j_3\rangle. \tag{4.28}$$

The scale and phase in (4.27) are the candidate coordinate normalization used by the finite validation suite.

*Numerical Check* 4.5 (Finite AS-coordinate validation). At the root orders $3 \leq k \leq 10$, direct evaluation at 50-digit working precision verifies, with residual below $10^{-30}$,

$$(B_n^U)^\dagger G B_n^U = G, \qquad A B^U A = \xi_k B^U A B^U, \tag{4.29}$$

the commuting-generator relations, the $S^3$ denominator, and the Poincaré vacuum ratio. The $k = 2$ theta space is one-dimensional and is checked separately. The independent negative-$E_8$ contraction checks the target at $2 \leq k \leq 12$.

These finite checks were reproduced from the recovered Wolfram Language engines for this candidate. The accompanying numerical reproducibility supplement contains the executable formulas, commands, and residual tables, including the separate one-dimensional case and a control omitting $\xi_k^8$. In the original theta coordinates the metric identity above is tested directly. Matrix products are also evaluated after conjugation by $G^{1/2}$, where $G^{1/2} B_n^U G^{-1/2}$ is unitary in the ordinary metric. Since the vacuum metric entry is one, this diagonal basis change does not alter the vacuum ratio. The negative-$E_8$/Habiro comparison and the Maslov prefix table are checked with exact cyclotomic and rational arithmetic, respectively; they are distinct from the 50-digit matrix tests.

*Remark* 4.6 (Limits of the AS-coordinate validation). The natural formal comparison would identify

$$S_{00} G^{1/2} B_n^{\mathrm{AS}} G^{-1/2} \quad \text{with a root-of-unity recoupling–twist–recoupling operator.}$$

Generic-$Q$ quantum-$6j$ orthogonality [7] does not by itself supply the exact Arthamonov–Shakirov-to-semisimplified-root dictionary, including truncation, the theta metric, the $S_{00}$ closure scalar, and the projective phase. We therefore do not claim an all-$k$ identification of the printed AS matrices with the canonical RT operator. No theorem below concerning Habiro descent, the compatible Habiro/disk lift, or closure uses such an identification; all of them use the canonical page-adapted extended RT gluing scalar directly.

4.5. **The Maslov lift of the five-chain coordinate candidate.** We spell out the exact integer calculation that fixes the nonlocal phase of the five-chain coordinate candidate, using Hansen's extended-TQFT Maslov convention [15]. In the ordered homology basis $(p_1, p_2, q_1, q_2)$ put

$$J = \begin{pmatrix} 0 & I_2 \\ -I_2 & 0 \end{pmatrix}, \qquad L = \operatorname{span}(p_1, p_2), \qquad \omega_{\mathrm{Tur}} = -J.$$

If $X_1, X_2, X_3$ are column bases of three Lagrangians, let $K = \ker[X_1 \ X_2 \ -X_3]$. Write $z = (a, b, c) \in K$, $x_2 = X_2 b$, and $x_3 = X_3 c$. The Kashiwara–Wall form is

$$q_K(z, z') = \frac{1}{2}\big(x_2^{\mathsf{T}} \omega_{\mathrm{Tur}} x_3' + (x_2')^{\mathsf{T}} \omega_{\mathrm{Tur}} x_3\big), \qquad \mu(X_1, X_2, X_3) = \operatorname{sign}(q_K). \tag{4.30}$$

Thus every entry below is computed as the signature of the rational symmetric form defined by (4.30), not by a floating-point or finite-level test. One nonzero form is displayed after the table.

For a curve vector $v$, the positive twist acts by $T_v = I_4 - vv^{\mathsf{T}} J$. The marked curves are

| | $A_1$ | $B_1$ | $A_2$ | $B_2$ | $A_3$ |
|---|---|---|---|---|---|
| $v$ | $(1,0,0,0)$ | $(0,0,1,0)$ | $(1,1,0,0)$ | $(0,0,0,1)$ | $(0,1,0,0)$. |

For a left-to-right word $h_1 \cdots h_m$, put $g_{r-1} = h_1 \cdots h_{r-1}$ and accumulate

$$\mu_r = \mu(h_r L, L, g_{r-1}^{-1} L). \tag{4.31}$$

Applying (4.30) to these integer matrices gives the complete prefix table

| word segment | successive Turaev cocycles | segment sum | cumulative sum |
|---|---|---|---|
| $I = A_1B_1A_2B_2A_3$ | $0,0,0,0,0$ | 0 | 0 |
| $(B_1A_2B_2A_2^{-1})_1$ | $0,0,0,0$ | 0 | 0 |
| $(B_1A_2B_2A_2^{-1})_2$ | $1,0,1,0$ | 2 | 2 |
| $(B_1A_2B_2A_2^{-1})_3$ | $1,0,1,0$ | 2 | 4 |
| $(B_1A_2B_2A_2^{-1})_4$ | $1,0,1,0$ | 2 | 6 |
| $(B_1A_2B_2A_2^{-1})_5$ | $1,0,1,0$ | 2 | 8 |

(4.32)

For example, the first nonzero entry is the initial $B_1$ in the second four-letter block. Its prefix is

$$g = B_1A_2B_2A_2^{-1} = \begin{pmatrix} 1 & -1 & -1 & -1 \\ 0 & 0 & -1 & -1 \\ 1 & -1 & 0 & -1 \\ 0 & 1 & 1 & 2 \end{pmatrix}.$$

For the three Lagrangians in (4.31), a nullspace basis of $[X_1 \ X_2 \ -X_3]$ is

$$(0,-1,0,1,0,0), \qquad (-1,1,2,0,1,1).$$

In that basis (4.30) is $\operatorname{diag}(0,2)$, so its signature is $+1$, as printed in the table. The remaining entries use the same integer calculation.

The same calculation gives weights 0 and 1 for $ABA$ and $BAB$, respectively, while their integral homology matrices agree. This is the exact braid-prefix sign calibration for the orientation convention $\omega_{\mathrm{Tur}} = -J$.

The Turaev composition law [15] has multiplier $\xi_k^{\mu}$. Summing the complete table gives

$$\mu_{\mathrm{Tur}}(I) = 0, \qquad \mu_{\mathrm{Tur}}(M_P^{\mathrm{five}}) = 8, \qquad I = A_1B_1A_2B_2A_3. \tag{4.33}$$

The genus-two five-chain construction in [3] identifies $I = A_1B_1A_2B_2A_3$ as the inversion that glues the two genus-two handlebodies to $S^3$; this is the geometric denominator for the separate theta-coordinate ratio. If $P_{\mathrm{RT}}^{\mathrm{proj}}(w)$ denotes the literal product of the canonical projective RT generators in Hansen's convention, the five-chain extended operators are

$$\rho_k^{\mathrm{five}}(M_P^{\mathrm{five}}) = \xi_k^8 P_{\mathrm{RT}}^{\mathrm{proj}}(M_P^{\mathrm{five}}), \qquad \rho_k^{\mathrm{five}}(I) = P_{\mathrm{RT}}^{\mathrm{proj}}(I). \tag{4.34}$$

**Theorem 4.7** (page-adapted finite Poincaré equality)**.** *For every $k \geq 2$, let $v^{+}_{\mathrm{sg},k}$ and $v^{-}_{\mathrm{sg},k}$ be the canonical state and dual cap functional (called a* cotest*) assigned to $H_{\mathrm{sg}}$ and $-H_{\mathrm{sg}}$, and let $\rho^{\mathrm{RT}}_{\mathrm{sg},k}(\widetilde{\Psi}_P)$ be the canonical extended RT operator assigned to the page-adapted mapping cylinder in (4.18); the tilde denotes the extended lift induced by that capped cobordism. Then the normalized gluing scalar satisfies*

$$\boxed{\frac{\langle v^{-}_{\mathrm{sg},k}, \rho^{\mathrm{RT}}_{\mathrm{sg},k}(\widetilde{\Psi}_P) v^{+}_{\mathrm{sg},k} \rangle_{\mathrm{ext}}}{Z^{\mathrm{RT}}_k(S^3)} = \tau_k(P).} \tag{4.35}$$

*Proof.* Proposition 4.3 identifies the capped page-adapted mapping cylinder with the oriented manifold $P$. The finite TQFT gluing axiom [5, §1.A] and Hansen's extended composition law [15] therefore identify the numerator with the extended RT partition function of that closed manifold. Division by the nonzero $S^3$ scalar gives the convention normalized by $\tau_k(S^3) = 1$. The argument applies at every $k \geq 2$ and uses neither a theta-vacuum cap nor the five-chain coordinate candidate. □

The independent finite target is the terminating Habiro expression [14]

$$\tau_k(P) = \frac{1}{1-Q} \sum_{m=1}^{k-1} Q^{m-1} (Q^m; Q)_m, \qquad Q = e^{2\pi i/k}. \tag{4.36}$$

Direct quantum-6$j$ evaluations at several discriminating levels agree with (4.36) and with an independent negative-$E_8$ contraction. Omitting the relative $\xi^8_k$ fails these tests. These checks detect errors in the candidate word, theta coordinate, orientation, or phase. The proof for every $k$ is instead Theorem 4.7 in the page-adapted marking.

The finite closed invariant comes from the page-adapted capped cobordism: $H_{\mathrm{sg}}$ and $\Psi_P$ specify the geometric self-gluing that produces $P$. The five-chain word $M^{\mathrm{five}}_P$, together with the phase and framing checks involving $\xi_k$ and $\mu_{\mathrm{Tur}}$, supplies independent finite-level validation coordinates. The compatible lift below is built from the finite invariant $\tau_k(P)$; it does not identify the two choices of cap data or turn the five-chain validation route into the geometric proof.

4.6. **The distinguished compatible lift.** Let

$$(Q)_n = \prod_{j=1}^{n} (1 - Q^j), \qquad \widehat{\mathbb{Z}[Q]} = \varprojlim_n \mathbb{Z}[Q]/((Q)_n) \tag{4.37}$$

be the Habiro completion. Evaluation at all roots of unity is injective, so Theorem 4.7 determines the Habiro component $J_P$. It does not yet determine a disk component.

For $P$ there is a distinguished larger completion

$$\mathcal{R} = \varprojlim_n \mathbb{Z}[Q]/\big(Q^n (Q)_n\big) \cong \widehat{\mathbb{Z}[Q]} \times \mathbb{Z}[[Q]]. \tag{4.38}$$

Indeed, $(Q)_n = \prod_{j=1}^{n}(1-Q^j) \equiv 1 \pmod{Q}$, so its image is a unit modulo $Q^n$. Thus the ideals $(Q^n)$ and $((Q)_n)$ are comaximal, and the finite Chinese remainder theorem gives compatible isomorphisms

$$\mathbb{Z}[Q]/\big(Q^n (Q)_n\big) \cong \mathbb{Z}[Q]/((Q)_n) \times \mathbb{Z}[Q]/(Q^n). \tag{4.39}$$

Passing to inverse limits gives the first factor as the Habiro completion and the second as $\mathbb{Z}[[Q]]$. Equivalently, in the two-parameter product system the diagonal is cofinal, since $n \geq \max\{a, b\}$ dominates the pair of levels $(a, b)$; this proves the displayed isomorphism. The product decomposition leaves the disk coordinate free: the Habiro coordinate alone does not

select it. The series below supplies the additional Poincaré-specific datum. Let $\pi_H$ and $\pi_0$ be the two projections. Define

$$h_m(Q) = Q^{m-1}\frac{(Q^m;Q)_m}{1-Q}, \qquad \widetilde{J}_P = \sum_{m\geq 1} h_m(Q). \tag{4.40}$$

Here is the divisibility needed for convergence. With $\Phi_1(Q) = Q-1$, cyclotomic factorization gives

$$(Q)_n = (-1)^n \prod_{d=1}^{n} \Phi_d(Q)^{\lfloor n/d\rfloor}, \qquad (Q^m;Q)_m = \prod_{r=m}^{2m-1}(1-Q^r). \tag{4.41}$$

For every $d \geq 2$, the interval $[m, 2m-1]$ of $m$ consecutive integers contains at least $\lfloor m/d\rfloor$ multiples of $d$. Hence, when $m \geq n+1$, the exponent of $\Phi_d$ in $(Q^m;Q)_m$ is at least $\lfloor m/d\rfloor \geq \lfloor n/d\rfloor$. There are $m$ factors $1-Q^r$ in that product, so division by $1-Q$ leaves $\Phi_1$ with exponent $m-1 \geq n$. Finally, the prefactor $Q^{m-1}$ is divisible by $Q^n$. Therefore

$$h_m(Q) \in Q^n(Q)_n \qquad (m \geq n+1), \tag{4.42}$$

and the sum converges in $\mathcal{R}$. Now set

$$\begin{aligned} \widetilde{B}_P &= 1 + Q(1-Q)\widetilde{J}_P \\ &= \sum_{m\geq 0} Q^m(Q^m;Q)_m. \end{aligned} \tag{4.43}$$

The Poincaré strange identity [16, 14] gives

$$\pi_H(\widetilde{J}_P) = J_P, \qquad \pi_0(\widetilde{B}_P) = A(Q). \tag{4.44}$$

**Theorem 4.8** (Poincaré joint compression)**.** *The affine compression of the distinguished lift*

$$\begin{aligned} \mathcal{C}_P(\widetilde{J}_P) &= Q^{-3/2}\left(1 + Q(Q-1)\pi_0(\widetilde{J}_P)\right) \\ &= Q^{-3/2}\left(2 - \pi_0(\widetilde{B}_P)\right) \end{aligned} \tag{4.45}$$

*equals*

$$\boxed{\mathcal{C}_P(\widetilde{J}_P) = Q^{-3/2}\big(2 - A(Q)\big) = \widehat{Z}_0(P;Q).} \tag{4.46}$$

*Proof.* We identify the two projections separately, using the root values for the Habiro coordinate and the specified series for the disk coordinate.

The divisibility above makes (4.40) and (4.43) well-defined in $\mathcal{R}$. Theorem 4.7 supplies their WRT root values, and Habiro's all-root injectivity identifies the Habiro projection with $J_P$. Apply the disk projection in (4.44), use the sourced oriented block of Theorem 3.1, and retain the exceptional endpoint of Proposition 3.2. These inputs give the displayed compression. □

4.7. **The closed Poincaré theorem and its scope.** The closing statement assembles three routes that have deliberately been proved separately. Page-adapted self-gluing supplies the all-level finite invariant, the five-chain coordinates provide a delimited finite validation, and the compatible Habiro/disk lift supplies the q-series compression. The three routes concern the same closed manifold but are not interchangeable: the finite tables do not replace the all-level gluing argument.

**Theorem 4.9** (Closed Poincaré realization)**.** *The page-adapted self-gluing in* (4.18) *gives* $\tau_k(P)$ *through the canonical extended RT functor for every root order* $k \geq 2$*. Separately, the five-chain coordinate candidate* $M_P^{\mathrm{five}} = (B_1A_2B_2A_2^{-1})^5$ *has exact relative Maslov weight* 8*, and*

*the normalized quantum-6j matrices supply the finite validation of Numerical Check 4.5; neither statement supplies an all-level page-cap-to-theta coordinate theorem. The resulting Habiro component has the distinguished compatible Habiro/disk lift (4.40), whose disk compression is*

$$\widehat{Z}_0(P;Q) = Q^{-3/2}\big(2 - A(Q)\big). \tag{4.47}$$

*Proof.* Proposition 4.1 reconstructs the marked genus-two surface and its integral intersection data; Proposition 4.2 identifies the marked diagram. Independently, Proposition 4.3 supplies the exact page-adapted decomposition. The extended TQFT gluing law then gives Theorem 4.7, hence the normalized equality with $\tau_k(P)$ for every $k \geq 2$. The five-chain word (4.22), its Maslov totals (4.33), and the finite quantum-6$j$ comparisons are validation data only, as stated in Remarks 4.4 and 4.6.

Those root values determine the Habiro component $J_P$ by Habiro's all-root injectivity theorem. Thus the compatible Habiro/disk lift uses the all-level finite WRT theorem. The divisibility $h_m \in Q^n(Q)_n$ for $m \geq n+1$ constructs the distinguished element $\widetilde{J}_P$ in the joint completion, and (4.44) identifies its two coordinates. Finally, Theorem 4.8, using the sourced oriented block and the exceptional endpoint of Proposition 3.2, computes its disk compression as $Q^{-3/2}(2 - A(Q))$. These are exactly the two assertions of the theorem. The finite validation checks test the candidate word, phase, orientation, endpoint, and printed AS coordinates. The ribbon, group, symplectic, Maslov, and finite-target checks are exact; the AS operator comparisons are high-precision numerical checks. No finite list of checks is used for the all-$k$ gluing implication. □

The source roles are distinct: the signed ribbon presentation comes from [17, 9]; the doubled-page cap from [19, 23]; the five-chain coordinates from [3]; the orientation dictionary from [4, 10]; the anomaly law from [15]; and the unified and endpoint inputs from [14, 18, 10].

## 5. Arbitrary-genus Gram sewing and Habiro scalar descent

The arbitrary-genus result is a closed-output theorem. It first contracts finite-root primal and cotest data to a scalar, then proves that the compatible scalars assemble into one Habiro element independent of the chosen Heegaard presentation. It does not assert the existence of a prime-independent boundary state. The order of construction is

$$\text{finite-root mapping cylinders} \longrightarrow \text{primal–cotest contraction}$$
$$\longrightarrow \text{closed WRT scalar} \longrightarrow \text{Habiro descent.}$$

Here *primal* means the state space and *cotest* means its chosen algebraic dual, as made explicit below. This order respects the distinction between finite-root boundary modules and closed scalars. The finite TQFT gluing, integral-lattice, and Heegaard inputs are those of [5, 8, 2]; the unified invariant and its specialization are those of [14]. In genus two the theta graph is primary, while higher-genus theta/ladder coordinates are used only as complete finite-root coordinate systems.

5.1. **The unimodular-$C$ Heegaard locus.** Let $H_g$ be the standard genus-$g$ handlebody, let $\Sigma_g = \partial H_g$, and fix the column-ordered symplectic basis

$$(a_1, \dots, a_g, b_1, \dots, b_g)$$

of $H_1(\Sigma_g;\mathbb{Z})$. The meridian Lagrangian is

$$L = \ker\big(H_1(\Sigma_g;\mathbb{Z}) \longrightarrow H_1(H_g;\mathbb{Z})\big) = \langle a_1, \dots, a_g\rangle.$$

For the oriented Heegaard gluing $M_\phi = H_g^- \cup_\phi H_g^+$, write the action on columns as

$$\phi_* = \begin{pmatrix} A_\phi & B_\phi \\ C_\phi & D_\phi \end{pmatrix} \in \mathrm{Sp}_{2g}(\mathbb{Z}).$$

The canonical homological calculation is the theorem on the homological data of the companion boundary-object paper [25, Theorem 2.5]. In the same fixed column convention it states

$$H_1(M_\phi;\mathbb{Z}) \cong \frac{H_1(\Sigma_g;\mathbb{Z})}{L+\phi_* L} \cong \frac{\mathbb{Z}^g}{C_\phi \mathbb{Z}^g} = \operatorname{coker} C_\phi \cong \operatorname{coker} C_\phi^{\mathsf{T}},$$

with row-to-column map $[u] \mapsto [D_\phi u]$. When $\det C_\phi \neq 0$, the same theorem gives $|H_1(M_\phi;\mathbb{Z})| = |\det C_\phi|$ and represents the row-coordinate linking form by $C_\phi^{-1} D_\phi \bmod \mathbb{Z}$. We use only the following closed-locus consequence.

**Corollary 5.1** (Integral-homology-sphere criterion)**.** *The closed manifold $M_\phi$ is an integral homology sphere if and only if $C_\phi \in \mathrm{GL}_g(\mathbb{Z})$, equivalently $\det C_\phi = \pm 1$.*

Suppose $h_-$ and $h_+$ extend over the two handlebodies. Their symplectic matrices have the form

$$h_\pm = \begin{pmatrix} P_\pm & Q_\pm \\ 0 & P_\pm^{-\mathsf{T}} \end{pmatrix}, \qquad P_\pm \in \mathrm{GL}_g(\mathbb{Z}).$$

**Proposition 5.2** (Double-coset stability of the homology criterion)**.** *One has*

$$C(h_- \phi h_+) = P_-^{-\mathsf{T}} C_\phi P_+.$$

*Thus the Smith type of* $\operatorname{coker} C_\phi$*, and in particular unimodularity, descends to the handlebody double coset.*

*Proof.* Block multiplication first gives $C(\phi h_+) = C_\phi P_+$, then $C(h_-\phi h_+) = P_-^{-\mathsf{T}} C_\phi P_+$. Both outside matrices are integrally unimodular, so they are precisely changes of presentation basis. □

*Remark* 5.3 (The $C$-block is not a three-manifold invariant). The matrix $C_\phi$ is only a presentation of first homology. Torelli mapping classes are invisible to the full symplectic matrix but can alter the glued manifold and its quantum invariants. No theorem below factors $J_{M_\phi}$, WRT, or the capped Heegaard scalar through $C_\phi$. Unimodularity specifies the domain of the scalar theorem; it does not classify the manifold.

5.2. **Finite-set polarized TQFT and exact sewing.** Let

$$\mathcal{P} = \{p : p \geq 5 \text{ is an odd prime}\}, \qquad \zeta_p = e^{2\pi i/p},$$
$$A_p^{\mathrm{std}} = i e^{2\pi i/(4p)}, \qquad (A_p^{\mathrm{std}})^4 = \zeta_p.$$

At the standard root, let the coefficient field $K_p^{\mathrm{std}}$ contain the modular data and let $V_{g,p}^{\mathrm{pr}}$ be the finite fusion-consistent trivalent-spine space. Its algebraic dual is

$$W_{g,p}^{\mathrm{ct}} = \mathrm{Hom}_{K_p^{\mathrm{std}}}(V_{g,p}^{\mathrm{pr}}, K_p^{\mathrm{std}}),$$

with evaluation $E_{g,p}(w,v) = w(v)$. The superscripts pr and ct distinguish the state and dual spaces; they do not identify either space with its conjugate. For a finite $F \subset \mathcal{P}$, take coordinatewise products

$$K_F^{\mathrm{std}} = \prod_{p\in F} K_p^{\mathrm{std}}, \quad V_{g,F}^{\mathrm{pr}} = \prod_{p\in F} V_{g,p}^{\mathrm{pr}}, \quad W_{g,F}^{\mathrm{ct}} = \prod_{p\in F} W_{g,p}^{\mathrm{ct}},$$

and let $E_{g,F}$ be the product pairing. The transition maps are coordinate deletions.

*Remark* 5.4 (The standard and Gilmer–Masbaum root conventions). The auxiliary Gilmer–Masbaum (GM) skein parameter is

$$q_p^{\mathrm{GM}} = (A_p^{\mathrm{std}})^2 = -e^{\pi i/p} = \zeta_p^{(p+1)/2}.$$

Its integral coefficient ring is

$$\mathcal{O}_p^{\mathrm{GM}} = \begin{cases} \mathbb{Z}[\zeta_p], & p \equiv -1 \pmod 4, \\ \mathbb{Z}[\zeta_{4p}], & p \equiv 1 \pmod 4. \end{cases}$$

If $\mathcal{S}_{g,p}^{\mathrm{GM}}$ is the free primal lattice, the correct integral cotest is

$$W_{g,p}^{\mathrm{GM,ct}} = \mathrm{Hom}_{\mathcal{O}_p^{\mathrm{GM}}}(\mathcal{S}_{g,p}^{\mathrm{GM}}, \mathcal{O}_p^{\mathrm{GM}}).$$

The Gilmer–Masbaum Hermitian gluing form identifies this cotest with the conjugate sharp dual; it is not generally the ordinary primal lattice of the oppositely oriented surface. Thus the GM branch has its own kernel

$$B_{\widetilde{\phi},p}^{\mathrm{GM}}(w,v) = E_{g,p}^{\mathrm{GM}}\big(w, \rho_{g,p}^{\mathrm{GM}}(\widetilde{\phi})v\big),$$

whereas $B_{\widetilde{\phi},p}^{\mathrm{Hdg}}$ below is defined directly in the standard Heegaard branch. We do not identify these uncontracted kernels or their state spaces. Their comparison is only between normalized closed scalars on the integral-homology-sphere locus.

The smallest exact root check fixes the substitution. At $p = 5$, the GM total-dimension formula gives

$$-\frac{5}{(\zeta_5 - \zeta_5^{-1})^2} = \frac{5-\sqrt{5}}{2}, \qquad -\frac{5}{(q_5^{\mathrm{GM}} - (q_5^{\mathrm{GM}})^{-1})^2} = \frac{5+\sqrt{5}}{2} = (\mathcal{D}_5^{\mathrm{Hdg}})^2.$$

Here $q_5^{\mathrm{GM}} = \zeta_5^3$. This checks which root enters the GM formula; it does not claim a dimension mismatch between the two branches.

**Proposition 5.5** (Finite-stage perfectness)**.** *For every finite $F$, the pairing $E_{g,F}$ is perfect over the product ring $K_F^{\mathrm{std}}$. Vacua, mapping-cylinder maps, pairings, and coefficient rings commute with every coordinate-deletion map. Hence the finite stages form an inverse system of polarized primal–cotest pairs.*

*Proof.* At one prime this is the defining finite-dimensional duality. The central idempotents of the finite product ring split every module into its $p$-components, so the product of the component duality isomorphisms is again an isomorphism. All remaining assertions are coordinatewise. The rank may vary with $p$; finite projectivity, not a fictitious constant rank, is the relevant statement. □

Keeping these inverse systems as pro-objects retains their finite-stage pairings and transition maps. Their set-theoretic inverse limits are

$$\varprojlim_F V_{g,F}^{\mathrm{pr}} = \prod_{p\in\mathcal{P}} V_{g,p}^{\mathrm{pr}}, \qquad \varprojlim_F W_{g,F}^{\mathrm{ct}} = \prod_{p\in\mathcal{P}} W_{g,p}^{\mathrm{ct}}.$$

The products are not thereby placed in perfect duality.

Let $\widetilde{\mathrm{MCG}}(\Sigma_g)$ be the Maslov/weight extension on which the finite TQFT acts honestly, and set

$$B_{\widetilde{\phi},p}^{\mathrm{Hdg}}(w,v) = E_{g,p}\big(w, \rho_{g,p}^{\mathrm{Hdg}}(\widetilde{\phi})v\big).$$

In finite fusion coordinates, denote the matrices of $E$, $\rho$, and $B$ by $e_{g,F}$, $r_{\widetilde{\phi},F}$, and $b_{\widetilde{\phi},F}$. Thus $b_{\widetilde{\phi},F} = e_{g,F} r_{\widetilde{\phi},F}$, componentwise. The superscript Hdg marks the direct Heegaard normalization.

**Theorem 5.6** (Finite-set polarized Gram sewing)**.** *For every finite $F$, every genus, and all composable lifted mapping cylinders,*

$$b_{\mathrm{id},F} = e_{g,F}, \qquad b_{\widetilde{\psi}\widetilde{\phi},F} = b_{\widetilde{\psi},F} e_{g,F}^{-1} b_{\widetilde{\phi},F}.$$

*These identities are covariant under independent complete fusion-tree coordinate changes and commute with coordinate deletion. They therefore give an exact pro-equality: equality at every finite stage, with no inverse metric on an infinite product.*

*Proof.* Inserting the inverse Gram matrix between the two pairing kernels recovers operator composition. This is why the middle pairing must be removed in the displayed product.

Functoriality gives $r_{\widetilde{\psi}\widetilde{\phi},F} = r_{\widetilde{\psi},F} r_{\widetilde{\phi},F}$. Hence

$$b_{\widetilde{\psi},F} e_{g,F}^{-1} b_{\widetilde{\phi},F} = e_{g,F} r_{\widetilde{\psi},F} e_{g,F}^{-1} e_{g,F} r_{\widetilde{\phi},F} = e_{g,F} r_{\widetilde{\psi},F} r_{\widetilde{\phi},F}.$$

The identity case is immediate. If primal and cotest coordinates change by $U$ and $X$, respectively, then

$$e' = X^{\mathsf{T}} e U, \qquad r' = U^{-1} r U, \qquad b' = X^{\mathsf{T}} b U;$$

substitution proves covariance. Everything is componentwise over $F$, so deletion preserves the identities. □

**Theorem 5.7** (Continuous duals of products and the inverse system)**.** *Finite-stage perfectness does not identify the pro-cotest $\prod_p W_{g,p}^{\mathrm{ct}}$ with the continuous scalar dual of $\prod_p V_{g,p}^{\mathrm{pr}}$. After embeddings of the coefficient fields in $\mathbb{C}$ and extension of scalars, every continuous linear functional on the product topology depends on only finitely many root coordinates, whereas the pro-cotest contains families with infinitely many nonzero coordinates.*

*Proof.* Finite duality does not pass to this infinite product: a continuous scalar functional can depend on only finitely many root coordinates.

Let $\ell$ be a continuous linear functional on the product. Continuity at zero gives a basic product neighborhood on which $\ell$ is bounded; such a neighborhood restricts only a finite coordinate set $F$. For a coordinate $p \notin F$, the entire $p$-th vector space lies in that neighborhood while all other coordinates vanish. Scaling that vector forces $\ell$ to vanish on the $p$-th coordinate. Hence $\ell$ has finite support. A product cotest with one nonzero component at every prime does not. Thus inverse Gram matrices in Theorem 5.6 can only mean finite-stage inverses. □

At genus two, every displayed finite-root kernel is written primarily in the theta basis. A complete quotient-first recoupling changes the primal basis and the cotest contragrediently, so the pairing and the kernel are unchanged. This is coordinate independence of an already-defined finite TQFT operator; it is not a single rational theta matrix specializing at all primes.

5.3. **Capping before descent.** Let $|0\rangle \in V_{g,p}^{\mathrm{pr}}$ be the positive handlebody vacuum and let $\langle 0| \in W_{g,p}^{\mathrm{ct}}$ be the normalized negative handlebody cotest. Write $\mathcal{D}_p$ for the total quantum dimension of the chosen finite-level theory. Keep anomaly and total-dimension factors in their one-dimensional normalization lines until contraction. For $g \geq 1$, define

$$\mathcal{A}_{g,p}^{\mathrm{std}}(\phi) = \mathcal{D}_p^{g-1} \langle 0 | \rho_{g,p}^{\mathrm{Hdg}}(\widetilde{\phi}) | 0 \rangle,$$

with the coherent lift/weight correction of the normalized TQFT, and set $\mathcal{A}_{0,p}^{\mathrm{std}}(S^3) = 1$.

**Theorem 5.8** (Finite-root capped Heegaard theorem)**.** *For every $p \in \mathcal{P}$ and every genus,*

$$\mathcal{A}_{g,p}^{\mathrm{std}}(\phi) = \mathrm{WRT}_p^{\mathrm{Hdg}}(M_\phi).$$

*The scalar is invariant under coherently normalized left and right handlebody actions, Heegaard stabilization and destabilization, and simultaneous contragredient theta/ladder transport. Its finite-root tuples commute with coordinate deletion.*

*Proof.* Apply the gluing axiom to the fully capped cylinder. The resulting identification, and the invariance checks below, concern closed scalars.

The Blanchet–Habegger–Masbaum–Vogel (BHMV) cobordism-composition axiom, the identification of the empty-surface space with the ground ring, and the interpretation of a closed

cobordism as a scalar [5, §1.A] identify the fully capped mapping cylinder with the normalized WRT invariant. Thus the normalized Heegaard definition is precisely the displayed vacuum coefficient; the Gram kernel makes the boundary contraction explicit. A mapping class extending over either handlebody only changes that handlebody's parameterization. Its central character is canceled by the inverse character in the normalization line. Stabilization glues in a canceling genus-one pair: the numerator and the normalized $S^3$ cap acquire the same local factor, so the quotient is unchanged. A complete basis change cancels between the primal and cotest. These are equalities of the fully contracted scalar, and all are rootwise. The integral lattices and complete fusion-coordinate realizations are those of [8, 2]. □

*Remark* 5.9 (Normalization away from the IHS locus). The superscript Hdg records the normalization of the direct Heegaard source. BHMV/GM conventions can carry an additional total-dimension power when $b_1 > 0$. The comparison below is made only on the integral-homology-sphere locus, where the normalized closed scalars agree; no equality of the two conventions is claimed for arbitrary closed three-manifolds.

The next two propositions are imported from the companion paper on integral root fibers and closed factorizations [24, Propositions 9.1–9.2]. They specify the closed cap used here; their proofs remain in that paper.

In those interfaces $M$ is an oriented integral homology sphere, $A = Q^{1/4}$, and the ordinary-skein cap is the full-IHS map of Garoufalidis–Lê, arXiv:2307.09135v2. The companion proof gives the fundamental-color sign, the linear extension and both Kauffman relations in this convention. Write $\mathscr{H} = \widehat{\mathbb{Z}[Q]}_{\mathrm{H}}$ for the ordinary Habiro ring. The integral target of this cap is $\mathscr{H}_A = \mathscr{H} \otimes_{\mathbb{Z}[Q^{\pm1}]} \mathbb{Z}[A^{\pm1}]$; its pure even source is only a $\mathbb{Z}[Q^{\pm1}]$-module. The generic pairing uses $\mathcal{K} = \mathscr{H}_A \otimes_{\mathbb{Z}[A^{\pm1}]} \mathbb{Q}(A^{1/2})$. Root evaluation is taken on $\mathscr{H}$ before this extension, not on the whole generic target.

The two further constructions in the comparison are the Lê–Murakami–Ohtsuki (LMO) invariant, whose $\mathfrak{sl}_2$ evaluation gives a perturbative closed scalar, and the Gelfand–Naimark–Segal (GNS) construction from the cap pairing. The *operational pairing* means the evaluation obtained by composing the geometric cap maps in the companion paper. Only their empty-skein values are compared here.

**Proposition 5.10** (Pure Habiro vacuum interface)**.** *For an integral homology sphere $M$, the ordinary-skein Habiro cap restricts on the even root-lattice sector to the ordinary Habiro ring, and the empty skein maps to $J_M$. At every root $\xi$, its value is Habiro's normalized $SU(2)$ WRT invariant. When the chosen fourth root $A = \xi^{1/4}$ is itself primitive of odd order, this agrees with the normalized $SO(3)$ sector. With $Q = e^h$, its expansion is the closed $\mathfrak{sl}_2$ LMO/Ohtsuki scalar.*

This is precisely the companion pure-vacuum proposition [24, Proposition 9.1]; it is a scalar cap statement, not an integral all-root boundary-state theorem.

**Proposition 5.11** (Operational/GNS vacuum interface)**.** *For an integral homology sphere, on the raw empty-skein geometric domain, after the companion coefficient inclusion from the Habiro ring into the companion coefficient extension $\mathcal{K}$, the operational pairing and the GNS pairing are the same scalar $J_M$. The identification reverses state/cotest variance through the same-oriented opposite equivalence: it interchanges the state and dual roles while keeping the orientation of the underlying manifold fixed. It uses neither orientation reversal of $M$ nor the substitution $Q \mapsto Q^{-1}$.*

This is precisely the companion operational-agreement proposition [24, Proposition 9.2]. It is not asserted to descend to the two variance-reversed radical quotients; such a descent would require a separate density or radical-comparison theorem.

**Lemma 5.12** (Odd-prime integral-homology-sphere bridge)**.** *If $C_\phi$ is unimodular, then*

$$\mathcal{A}^{\mathrm{std}}_{g,p}(\phi) = \tau'_p(M_\phi) = \tau_{\zeta_p}(M_\phi),$$

*where $\tau'_p$ is the odd-level $SO(3)$ invariant and $\tau_{\zeta_p}$ is Habiro's $sl_2$-normalized scalar.*

*Proof.* Corollary 5.1 puts $M_\phi$ on the integral homology-sphere locus. In the standard root convention, the normalized Heegaard $SO(3)$ formula equals its surgery formula. Habiro's odd-level comparison theorem [14] identifies that surgery scalar with $\tau_{\zeta_p}$, with $S^3 = 1$. Every comparison is made after both boundary caps have been contracted. □

For later comparison with the physical/common GM branch, define only at the scalar level

$$\sigma_p(\zeta_p) = \zeta_p^{(p+1)/2}, \qquad q_p^{\mathrm{com}} = \sigma_p(\zeta_p), \qquad \mathcal{A}^{\mathrm{com}}_{g,p} = \sigma_p(\mathcal{A}^{\mathrm{std}}_{g,p}).$$

Then $\sigma_p^{-1}(\mathcal{A}^{\mathrm{com}}_{g,p}) = \mathcal{A}^{\mathrm{std}}_{g,p}$. No state-space intertwiner is asserted: the automorphism is applied only after both boundary caps have been contracted.

5.4. **The arbitrary-genus Habiro scalar.** Recall

$$\widehat{\mathbb{Z}[Q]}_{\mathrm{H}} = \varprojlim_N \mathbb{Z}[Q]/((Q)_N), \qquad (Q)_N = \prod_{j=1}^{N}(1-Q^j).$$

Polynomial evaluation at any root of unity $\xi$ extends to a map $\mathrm{Ev}_\xi : \widehat{\mathbb{Z}[Q]}_{\mathrm{H}} \to \mathbb{Z}[\xi]$.

**Theorem 5.13** (Arbitrary-genus Heegaard–Habiro scalar descent)**.** *Let $g \geq 0$ and let $\phi \in \mathrm{MCG}(\Sigma_g)$ have unimodular block $C_\phi$. There is a unique scalar*

$$\mathfrak{Z}^{\mathrm{cyc}}_g(\phi) := J_{M_\phi} \in \widehat{\mathbb{Z}[Q]}_{\mathrm{H}}$$

*such that, for every root of unity $\xi$,*

$$\mathrm{Ev}_\xi\, \mathfrak{Z}^{\mathrm{cyc}}_g(\phi) = \tau_\xi(M_\phi).$$

*At every odd prime $p \geq 5$,*

$$\mathrm{Ev}_{\zeta_p}\, J_{M_\phi} = \mathcal{A}^{\mathrm{std}}_{g,p}(\phi) = \sigma_p^{-1}\big(\mathcal{A}^{\mathrm{com}}_{g,p}(\phi)\big).$$

*The family of primitive odd-prime values already determines $J_{M_\phi}$ uniquely.*

*Proof.* The construction has an existence half and a uniqueness half. Habiro's admissible surgery presentation gives a convergent cyclotomic element and presentation independence makes it topological; the capped Heegaard bridge identifies its odd-prime values. Uniqueness is a separate limit-point argument in the Habiro topology, not an interpolation assertion in the product of root fields.

By Corollary 5.1, $M_\phi$ is an integral homology sphere. Choose Habiro's admissible presentation [14] by an algebraically split link $L = L_1 \cup \cdots \cup L_m$ with framings $f_i \in \{\pm 1\}$. If $L^0$ is the zero-framed link and $\omega^{-f_i}$ is Habiro's surgery color for the framing $f_i$, set

$$J_{M_\phi} = J_{L^0}(\omega^{-f_1}, \ldots, \omega^{-f_m}).$$

Habiro's colored-link divisibility makes this series converge in the cyclotomic completion [14]. The twist-functional identity and Hoste-move theorem in the same source make it independent of the admissible presentation, and its specialization theorem gives $\mathrm{Ev}_\xi\, J_{M_\phi} = \tau_\xi(M_\phi)$ at every root. Proposition 5.10 identifies this same element with the empty-skein closed cap; Proposition 5.11 identifies the raw operational and GNS vacuum coefficients with it, without changing orientation or inverting $Q$. The unimodularity criterion verifies the IHS hypothesis of both imported interfaces, and the comparison is on empty skeins before either radical quotient. This cap identification uses the companion's signed ordinary-skein map; the existence and all-root specialization above use Habiro's unified closed invariant independently. Lemma 5.12 supplies the capped Heegaard equality; Galois naturality is applied only after contraction.

For uniqueness from odd primes, let $S = \{\zeta_p : p \in \mathcal{P}\}$. In Habiro's adjacency topology every $\zeta_p$ is adjacent to 1, because its quotient by 1 has prime order. Hence 1 is a limit point of $S$. Habiro's limit-point injectivity theorem [14] makes

$$\widehat{\mathbb{Z}[Q]}_{\mathrm{H}} \longrightarrow \prod_{p\in\mathcal{P}} \mathbb{Z}[\zeta_p]$$

injective. Therefore the primitive-prime values determine the scalar. □

**Corollary 5.14** (Topological descent and elementary operations)**.** *On the unimodular-C locus, $\mathfrak{Z}_g^{\mathrm{cyc}}$ is invariant under handlebody double cosets and Heegaard stabilization. It depends only on the oriented integral homology sphere and satisfies*

$$J_{M\#N} = J_M J_N, \qquad J_{S^3} = 1, \qquad J_{-M}(Q) = J_M(Q^{-1}).$$

*Proof.* Double-coset moves and stabilization preserve the oriented glued manifold, and the unified invariant is presentation independent. The three formulas are respectively Habiro's connected-sum, normalization, and orientation identities [14]. □

*Remark* 5.15 (Root-product existence is not Habiro coherence). The target $\prod_p \mathbb{Z}[\zeta_p]$ is larger than the image used in Theorem 5.13. Arbitrary finite prime interpolation does not prove that a root tuple comes from one Habiro element. Existence here follows from the unified invariant of the closed manifold; uniqueness then follows from limit-point injectivity.

### 5.5. **Literal common cyclotomic and Taylor approximants.**

**Lemma 5.16** (Successive Habiro lifting)**.** *Every $f \in \widehat{\mathbb{Z}[Q]}_{\mathrm{H}}$ admits an expansion*

$$f(Q) = \sum_{n=0}^{\infty} f_n(Q)(Q)_n, \qquad f_n(Q) \in \mathbb{Z}[Q].$$

*Proof.* Inductively choose a polynomial representative modulo $((Q)_N)$.

If $P_N = \sum_{n<N} f_n(Q)(Q)_n$ represents the $N$-th coordinate, then a representative at level $N+1$ differs from $P_N$, modulo $((Q)_{N+1})$, by a multiple $f_N(Q)(Q)_N$, because $((Q)_N)$ is principal. The compatible partial sums define $f$. □

Fix such an expansion and put

$$P_N(f;Q) = \sum_{n=0}^{N-1} f_n(Q)(Q)_n \in \mathbb{Z}[Q].$$

Let $\iota_1 : \widehat{\mathbb{Z}[Q]}_{\mathrm{H}} \to \mathbb{Z}[[Q-1]]$ be the Taylor expansion map at $Q = 1$.

**Theorem 5.17** (Common cyclotomic–Ohtsuki approximants)**.** *The same polynomial $P_N(f;Q)$ satisfies both:*

*(1) if $\xi$ has order $r \le N$, then $P_N(f;\xi) = \mathrm{Ev}_\xi(f)$;*

*(2) at $Q = 1$,*

$$\iota_1(f) - P_N(f;Q) \in (Q-1)^N \mathbb{Z}[[Q-1]].$$

*For $f = J_{M_\phi}$, the Taylor coordinate is the Ohtsuki series. Thus every integral-homology-sphere Heegaard word, in every genus, has one polynomial sequence simultaneously giving exact values on growing finite root sets and growing Taylor accuracy.*

*Proof.* Both approximation properties follow from the same omitted tail. For $n \ge r$, the factor $1 - Q^r$ occurs in $(Q)_n$, so every omitted term vanishes at an $r$-th root. Each of the $n$ factors of $(Q)_n$ is divisible by $Q-1$, so the tail beginning at $n = N$ has Taylor order at least $N$. Habiro's Taylor theorem [14] identifies $\iota_1(J_M)$ with the Ohtsuki series. □

*Remark* 5.18 (Habiro descent does not imply disk convergence). The construction above does not by itself supply a $Q$-adically convergent series at $Q = 0$ for a general integral homology sphere, nor does it prove that the approximants $P_N$ are $Q$-adically Cauchy. Every cyclotomic factor $(Q)_n$ has constant term 1. Therefore the filtration forcing convergence in the Habiro completion does not force the orders at $Q = 0$ to increase. A separate argument is required for any manifold-specific disk series. The genuine global impossibility theorem for a continuous polynomial-preserving map from the whole Habiro ring to $\mathbb{Z}[[Q]]$ is Corollary 6.12.

*Remark* 5.19 (What the arbitrary-genus theorem closes). The arbitrary-genus closed scalar, its double-coset and stabilization descent, and its common cyclotomic–Ohtsuki approximants are proved on the unimodular-$C$ locus. This does not construct a strict all-prime longitude-twist boundary state, an infinite-product Riesz duality, a generic-$Q$ handlebody state, a non-IHS vector of Spin$^c$ blocks, or a disk function. Those are logically separate questions.

## 6. Radial comparison with plumbing $\widehat{Z}$

The closed scalar is now available. On a specified negative-definite plumbing class, an independently defined disk block has a radial endpoint that can be compared with it. After matching the conventions, we show why even these endpoints do not determine the disk series. The comparison gives no map from the Habiro ring to disk series.

The proof combines the arbitrary-genus scalar descent of Section 5 with the analytic radial theorem of [22]. The convention match is checked against [12, 10, 14]. No formal interchange of a root limit and an unsourced infinite sum is used.

6.1. **The exact plumbing and radial hypotheses.** Let $\Gamma = (V, E, (w_v)_{v\in V})$ be a finite weighted tree and let its intersection matrix be

$$W_{vv} = w_v, \qquad W_{uv} = \begin{cases} 1, & \{u, v\} \in E, \\ 0, & \{u, v\} \notin E. \end{cases}$$

The oriented manifold $M(\Gamma)$ is the surgery-oriented boundary of the corresponding four-dimensional plumbing. Throughout the positive radial theorem, assume

$$W < 0, \qquad \det W = \pm 1.$$

It follows that $M(\Gamma)$ is an integral homology sphere.

For $v \in V$, write

$$\overline{v} = \{u : \{u, v\} \in E,\ \deg(u) = 1\}, \qquad V_{\geq 3} = \{v : \deg(v) \geq 3\}.$$

The analytic hypothesis is exactly

$$|\overline{v}| + 2 - \deg(v) > 0 \qquad (v \in V_{\geq 3}). \tag{6.1}$$

It is not the stronger nearby figure condition that quantifies over all vertices.

A concrete four-vertex test. The example used below is the star with one central vertex and three leaves. Its plumbing matrix is small enough that definiteness and unimodularity can be checked directly, and it displays the comparison at issue: the same closed manifold has a finite-root scalar, an all-root Habiro element, and a radial value of an independently defined disk block. The matrix check supplies the topological hypotheses; the radial theorem is the separate step that relates the disk endpoint to the closed scalar. Thus the example illustrates the output chain without suggesting a general map from Habiro elements to disk series.

For $k \geq 3$, put

$$\zeta_k = e^{2\pi i/k}, \qquad Q_k(t) = \zeta_k e^{-t} \quad (t > 0),$$

and freeze the lifted logarithm

$$\log Q_k(t) = \frac{2\pi i}{k} - t.$$

Thus $Q_k(t)^{1/2} = \zeta_{2k} e^{-t/2}$. Every fractional power below uses this lift, and

$$\mathrm{Rad}_{Q\to\zeta_k} F(Q) = \lim_{t\downarrow 0} F(Q_k(t)).$$

6.2. **The two normalization bridges.** Let $\mathrm{WRT}_k^{\mathrm{Mur}}$ denote Murakami's normalized invariant [22], and let $\tau_{\zeta_k}^{\mathrm{Hab}}$ be Habiro's $sl_2$ normalization [14].

**Lemma 6.1** (WRT convention bridge)**.** *With*

$$Q = \zeta_k, \qquad Q^{1/2} = \zeta_{2k}, \qquad Q^{1/4} = \zeta_{4k},$$

*one has, for every integral homology sphere $Y$,*

$$\mathrm{WRT}_k^{\mathrm{Mur}}(Y) = \tau_{\zeta_k}^{\mathrm{Hab}}(Y).$$

*Proof.* Murakami's plumbing formula uses the surgery normalization of Gukov–Pei–Putrov–Vafa [12, 22]. Its colors are $n = 1, \dots, k-1$, its quantum dimension is

$$[n] = \frac{Q^{n/2} - Q^{-n/2}}{Q^{1/2} - Q^{-1/2}},$$

and its framing eigenvalue is $Q^{(n^2-1)/4}$. Habiro's Kirby color is $\Omega_k = \sum_{i=0}^{k-2} [i+1] V_i$, its twist on $V_i$ is $Q^{i(i+2)/4}$, and its surgery value is divided by the same evaluations of the $+1$- and $-1$-framed Kirby-colored unknots. Under $n = i+1$, the colors, dimensions, twists, inertia normalizations, and surgery orientation agree term by term. On an integral homology sphere the fourth-root choice drops out, so the normalized scalars coincide. □

Let $\widehat{Z}_\Gamma$ denote Murakami's plumbing block [22], and let $\widehat{Z}_0$ denote the unique IHS block in the convention of Gukov–Manolescu [10].

**Lemma 6.2** (Plumbing-block convention bridge)**.** *For a negative-definite unimodular plumbing tree,*

$$\widehat{Z}_\Gamma(Q) = \widehat{Z}_0(M(\Gamma); Q)$$

*with the full monomial prefactor and with exactly one factor $2^{-|V|}$.*

*Proof.* Put $s = |V|$. The coefficient-sum formula of Gukov–Manolescu [10] has prefactor

$$2^{-s}(-1)^{\pi} Q^{(3\sigma - \sum_v w_v)/4}.$$

Here $\pi$ is the number of positive eigenvalues of $W$ and $\sigma$ is its signature. Negative definiteness gives $\pi = 0$ and $\sigma = -s$, so this becomes

$$2^{-s} Q^{-\sum_v (w_v+3)/4},$$

which is the Murakami prefactor. Both coefficient-sum formulas use the sum of the inner and outer Laurent expansions in every variable. In the contour form, the Gukov–Manolescu principal value is averaged; Murakami uses the unaveraged sum and compensates by the displayed $2^{-s}$. Hence no second factor is present. Finally, unimodularity gives $W\mathbb{Z}^V = \mathbb{Z}^V$, so the sole theta coset $2W\mathbb{Z}^V + a$, $a \equiv \delta \pmod 2$, is $2\mathbb{Z}^V + \delta$, exactly the lattice in the Murakami definition. The vector $\delta$ records the vertex degrees, and $a$ is a representative of the block's parity class. □

**Theorem 6.3** (Murakami radial theorem in the fixed conventions)**.** *If $W < 0$, $\det W = \pm 1$, and (6.1) holds, then for every $k \geq 3$,*

$$\mathrm{WRT}_k^{\mathrm{Mur}}(M(\Gamma)) = \frac{\mathrm{Rad}_{Q\to\zeta_k} \widehat{Z}_\Gamma(Q)}{2(\zeta_{2k} - \zeta_{2k}^{-1})}.$$

*Proof.* This is [22, Theorem 1.2 and Corollary 6.4]. That theorem assumes a negative-definite unimodular tree and states the leaf condition precisely for $v \in V_{\geq 3}$. Lemma 6.1 fixes the closed-scalar normalization and root, while Lemma 6.2 fixes the disk block and its single $2^{-s}$ factor. These substitutions give the displayed formula without an additional normalization constant. □

*Remark* 6.4 (No unsourced exchange of limit and sum). The derivation in [12, Appendix A, equations (A.27)–(A.28)] assumes the indicated interchange of regularization and root limits; that assumption is not a proof input here. Murakami subsequently proved the weighted radial relation for general negative-definite plumbing trees [21, Theorem 1.2]. The analytic input to our comparison remains Theorem 6.3, with its declared plumbing hypotheses.

More precisely, the later theorem allows nonunimodular linking matrices and removes the leaf condition. Its radial limit is taken *after* the finite weighted sum over plumbing labels; it does not assert that each individual block has a radial limit. On the unimodular locus there is one block label, so this distinction disappears, but we do not enlarge the theorems below. The closed scalar, fractional-power lift, and block normalization remain those fixed by the two preceding convention bridges.

6.3. **The arbitrary-genus radial comparison.** The preceding theorem supplies the analytic radial endpoint for one plumbing presentation. The next theorem changes only the topological presentation: the same closed manifold is represented by an arbitrary-genus Heegaard word, and its closed invariant is carried through the Habiro specialization to the Heegaard scalar. No new radial convergence statement is introduced here; the plumbing hypotheses remain in force while the Heegaard genus and splitting are allowed to vary.

**Theorem 6.5** (Heegaard–Habiro–$\widehat{Z}$ radial comparison)**.** *Let $\Gamma$ satisfy the hypotheses of Theorem 6.3. Let $\phi$ be any genus-$g$ Heegaard word and fix an orientation-preserving diffeomorphism*

$$M_\phi \cong M(\Gamma).$$

*Then $C_\phi$ is unimodular and, for every $k \geq 3$,*

$$\boxed{\mathrm{Rad}_{Q\to\zeta_k}\,\widehat{Z}_\Gamma(Q) = 2(\zeta_{2k} - \zeta_{2k}^{-1})\,\mathrm{Ev}_{\zeta_k}\,\mathfrak{Z}_g^{\mathrm{cyc}}(\phi).}$$

*At every odd prime $p \geq 5$, this is*

$$\boxed{\mathrm{Rad}_{Q\to\zeta_p}\,\widehat{Z}_\Gamma(Q) = 2(\zeta_{2p} - \zeta_{2p}^{-1})\mathcal{A}_{g,p}^{\mathrm{std}}(\phi).}$$

*Both identities are independent of the genus and of the chosen Heegaard splitting.*

*Proof.* Follow the invariant through a closed-scalar chain: plumbing block to WRT, orientation-preserving identification to the Heegaard manifold, and Habiro specialization to the finite-root Heegaard scalar. The prime-level formula uses the separate odd-prime bridge. Since every step is a closed invariant identity, genus and splitting choices disappear only after contraction.

The plumbing is unimodular, so its boundary is an integral homology sphere; Corollary 5.1 therefore makes $C_\phi$ unimodular. The orientation-preserving identification, Lemma 6.1, the radial source theorem, and Habiro specialization give the chain of exact closed-scalar equalities

$$\frac{\mathrm{Rad}_{Q\to\zeta_k}\,\widehat{Z}_\Gamma(Q)}{2(\zeta_{2k} - \zeta_{2k}^{-1})} = \tau_{\zeta_k}(M(\Gamma)) = \tau_{\zeta_k}(M_\phi) = \mathrm{Ev}_{\zeta_k}\,J_{M_\phi}.$$

The denominator is nonzero for $k \geq 3$, which proves the first formula. At an odd prime, apply Lemma 5.12 for the second. Habiro's scalar and normalized WRT depend only on the oriented closed manifold, and Corollary 5.14 gives explicit double-coset and stabilization descent. Thus the result is independent of the Heegaard genus. □

**Corollary 6.6** (Radial endpoint invariance)**.** *If* $\Gamma$ *and* $\Gamma'$ *both satisfy the hypotheses and bound the same oriented integral homology sphere, then, for every* $k \geq 3$*,*

$$\mathrm{Rad}_{Q\to\zeta_k}\widehat{Z}_\Gamma(Q) = \mathrm{Rad}_{Q\to\zeta_k}\widehat{Z}_{\Gamma'}(Q).$$

*Proof.* Apply Theorem 6.5 to both plumbings. The right side is the same multiple of the same Habiro evaluation. □

The corollary identifies radial endpoints, not the two disk series. Proposition 6.11 below shows why the latter inference is false.

6.4. **The non-Poincaré witness** $\Sigma(2,3,7)$**.** Consider the star-shaped plumbing with central weight $-1$ and leaf weights $-2,-3,-7$:

$$W_{237} = \begin{pmatrix} -1 & 1 & 1 & 1 \\ 1 & -2 & 0 & 0 \\ 1 & 0 & -3 & 0 \\ 1 & 0 & 0 & -7 \end{pmatrix}.$$

With the fixed surgery orientation its boundary is $\Sigma(2,3,7) = S^3_{-1}(T_{2,3})$.

**Lemma 6.7** (The $\Sigma(2,3,7)$ plumbing hypotheses)**.** *The matrix* $W_{237}$ *is negative definite, has determinant* 1*, and its graph satisfies* (6.1)*.*

*Proof.* Let $D = \mathrm{diag}(-2,-3,-7)$. Its Schur complement in $W_{237}$ is

$$-1-(1,1,1)D^{-1}(1,1,1)^{\mathsf{T}} = -1+\frac{1}{2}+\frac{1}{3}+\frac{1}{7} = -\frac{1}{42}.$$

Since $D<0$ and the complement is negative, the Schur-complement criterion gives $W_{237}<0$. Moreover

$$\det W_{237} = \det(D)(-1/42) = (-42)(-1/42) = 1.$$

The only vertex of degree at least three is the center. It has three adjacent leaves and degree three, so its leaf quantity is $3+2-3=2>0$. □

**Corollary 6.8** (Arbitrary-genus $\Sigma(2,3,7)$ comparison)**.** *For any orientation-compatible genus-*$g$ *presentation* $M_\phi \cong \Sigma(2,3,7)$ *and every odd prime* $p \geq 5$*,*

$$\mathrm{Rad}_{Q\to\zeta_p}\widehat{Z}_0(\Sigma(2,3,7);Q) = 2(\zeta_{2p}-\zeta_{2p}^{-1})\mathcal{D}_p^{g-1}\langle 0|\rho_{g,p}^{\mathrm{Hdg}}(\widetilde{\phi})|0\rangle.$$

*In the fixed branch, the full block begins*

$$\widehat{Z}_0(\Sigma(2,3,7);Q) = Q^{1/2}(1-Q-Q^5+Q^{10}-Q^{11}+Q^{18}+Q^{30}-Q^{41}+\cdots).$$

*Proof.* Lemma 6.7 verifies every hypothesis of Theorem 6.5. Applying that theorem and then expanding the definition of $\mathcal{A}^{\mathrm{std}}_{g,p}$ gives the first formula. The plumbing-block convention bridge identifies the disk series with the unique IHS block $\widehat{Z}_0$. Substitution of the eight nonzero residue classes modulo 84 in the coefficient-sum formula gives exponents $0,1,5,10,11,18,30,41$ and signs $+,-,-,+,-,+,+,-$, proving the displayed initial expansion with its $Q^{1/2}$ prefactor. □

The full monomial normalization is essential. If

$$F_{\mathrm{mock}7}(Q) = Q^{1/168}(1-Q-Q^5+\cdots),$$

then

$$\widehat{Z}_0 = Q^{83/168}F_{\mathrm{mock}7}, \qquad \frac{83}{168}+\frac{1}{168} = \frac{1}{2}.$$

The additive exceptional term in the Brieskorn decomposition occurs for $\Sigma(2,3,5)$, not for $\Sigma(2,3,7)$; the latter is the pure false-theta branch.

6.5. **The exact Bailey matched-order lift.** The subsection follows one concrete closed-manifold witness from topology to analysis. The verified plumbing data first identify the normalized false-theta block; the periodic character and finite Bailey kernel then give an exact polynomial identity at roots of unity. A separate radial theorem turns that identity into the endpoint formula, while the order-two and order-three residue tests are kept afterward as an obstruction to treating the matched finite polynomials as one common projective tower.

Let $\chi : \mathbb{Z} \to \{-1, 0, 1\}$ have period 84, with

$$\chi(n) = +1 \quad (n \equiv 1, 41, 55, 71 \pmod{84}),$$
$$\chi(n) = -1 \quad (n \equiv 13, 29, 43, 83 \pmod{84}),$$

and zero otherwise. Put

$$F(Q) = \sum_{n \geq 0} \chi(n) Q^{(n^2-1)/168}, \qquad \widehat{Z}_0(\Sigma(2,3,7); Q) = Q^{1/2} F(Q).$$

For a primitive root $\zeta_N^M$, $(M, N) = 1$, the radial branch is

$$Q = \exp(2\pi i M/N - t), \qquad \log Q = 2\pi i M/N - t.$$

In particular, $(\zeta_N^M)^{1/2}$ below means $e^{\pi i M/N}$.

**Theorem 6.9** (Exact 237 Bailey endpoint identity)**.** *Define the Hikami–Habiro series* [16, 20] *by*

$$H(Q) = \sum_{n \geq 0} Q^{-n(n+2)} (Q^{n+1}; Q)_{n+1} = (1 - Q) J_{\Sigma(2,3,7)}(Q)$$

*and*

$$F_N(Q) = \sum_{0 \leq n \leq 14N} \chi(n) Q^{(n^2-1)/168}.$$

*The specialized finite Bailey identity also gives the literal polynomial formula*

$$F_N(Q) = \sum_{k=0}^{N-1} s_k(Q),$$
$$s_k(Q) = \begin{cases} 0, & k \equiv 1 \pmod 3, \\ (-1)^{k + \lfloor (4k+1)/3 \rfloor} Q^{(7k^2+k)/6} (1 - Q^{2k+1}), & k \not\equiv 1 \pmod 3. \end{cases} \tag{6.2}$$

*Then, for every primitive* $\zeta_N^M$,

$$F_N(\zeta_N^M) = -(\zeta_N^M)^{-1} H(\zeta_N^M),$$

*and*

$$\mathrm{Rad}_{Q \to \zeta_N^M} F(Q) = -2(\zeta_N^M)^{-1} H(\zeta_N^M).$$

*Consequently*

$$\mathrm{Rad}_{Q \to \zeta_N^M} \widehat{Z}_0(Q) = 2\big((\zeta_N^M)^{1/2} - (\zeta_N^M)^{-1/2}\big) \operatorname{Ev}_{\zeta_N^M} J_{\Sigma(2,3,7)}.$$

*Proof.* The finite Bailey identity fixes the endpoint kernel; the plumbing formula fixes the block prefactor. We keep these two normalizations separate until the final factorization.

The Bailey pair and its polynomial identity in [20], specialized to its parameter $p = 1$, give the finite matched-order equality. The theorem and its displayed Eichler-integral identity in the same source identify

$$\widetilde{\Phi}^{(1,1,1)}_{(2,3,7)}(\tau) = Q^{1/168} F(Q)$$

and its radial theorem gives the second equality on the declared lifted cusp. The plumbing-block formula of [10, Proposition 4.8, equation (56), and Table 1] identifies $Q^{1/2}F$ with the full block. Finally,

$$-2Q^{-1/2} H(Q) = -2Q^{-1/2}(1 - Q) J(Q) = 2(Q^{1/2} - Q^{-1/2}) J(Q),$$

which proves the last formula with no unfixed square-root sign. □

For a sequence of polynomials to converge in the Habiro completion, its residue must eventually stabilize modulo every fixed $(Q)_n$. Agreement only at the root whose order matches the truncation index does not imply this compatibility.

**Theorem 6.10** (The raw Bailey family is not a common projective tower)**.** *The full sequence $F_N$ is not Cauchy in the Habiro topology. No subsequence has the required coordinate $-Q^{-1}H(Q)$ eventually at both the roots of orders 2 and 3. Thus the matched-order identity does not itself produce common cyclotomic approximants.*

Two root coordinates obstruct a common tower. To disprove a common projective tower, it is enough to inspect two root coordinates of the exact finite kernel. Translation gives a periodic summand sequence at each root; the cumulative tables show that the required order-two and order-three residues occur in disjoint congruence classes. This obstructs eventual correctness at both roots simultaneously. It leaves open the possibility of subsequences that stabilize to other values.

*Proof. The order-two root test.* We use the exact kernel (6.2). At $Q = -1$, translation by 12 preserves the support condition, changes the sign exponent by $12+16 = 28$, changes $(7k^2+k)/6$ by $28k + 170$, and changes $2k + 1$ by 24. Hence $s_{k+12}(-1) = s_k(-1)$. The twelve summands are

$$2, 0, 2, 2, 0, 2, -2, 0, -2, -2, 0, -2,$$

whose sum is zero. Their cumulative sums give the complete exact table

(6.3)

| $N \bmod 12$ | 0 | 1 | 2 | 3 | 4 | 5 | 6 | 7 | 8 | 9 | 10 | 11 |
|---|---|---|---|---|---|---|---|---|---|---|---|---|
| $F_N(-1)$ | 0 | 2 | 2 | 4 | 6 | 6 | 8 | 6 | 6 | 4 | 2 | 2. |

Thus the value is the required $F_2(-1) = 2$ precisely for

$$N \bmod 12 \in \{1, 2, 10, 11\}.$$

*The order-three root test.* Now let $\omega^2 + \omega + 1 = 0$. Translation by 18 changes the sign exponent by $18 + 24 = 42$, changes $(7k^2 + k)/6$ by $42k + 381$, a multiple of 3, and changes $2k+1$ by 36. Therefore $s_{k+18}(\omega) = s_k(\omega)$. Direct reduction of this one symbolic 18-term block has zero sum, and its cumulative sums are

(6.4)

| $N \bmod 18$ | 0 | 1 | 2 | 3 | 4 | 5 |
|---|---|---|---|---|---|---|
| $F_N(\omega)$ | 0 | $1-\omega$ | $1-\omega$ | $2+\omega$ | $4+2\omega$ | $4+2\omega$ |
| $N \bmod 18$ | 6 | 7 | 8 | 9 | 10 | 11 |
| $F_N(\omega)$ | $6+3\omega$ | $7+5\omega$ | $7+5\omega$ | $8+4\omega$ | $7+5\omega$ | $7+5\omega$ |
| $N \bmod 18$ | 12 | 13 | 14 | 15 | 16 | 17 |
| $F_N(\omega)$ | $6+3\omega$ | $4+2\omega$ | $4+2\omega$ | $2+\omega$ | $1-\omega$ | $1-\omega$. |

The cycle returns to zero at $N \equiv 0 \pmod{18}$. The required primitive cube-root value is $F_3(\omega) = 2 + \omega$, attained precisely for

$$N \bmod 18 \in \{3, 15\}.$$

*Incompatible congruence classes.* Every member of the second set is 3 or 9 (mod 12), disjoint from the first set. Therefore no subsequence is eventually correct at both roots. The nonconstant order-two cycle also prevents the full sequence from being Habiro-Cauchy, since evaluation at a fixed root is eventually constant for every Habiro-Cauchy sequence. All reductions above take place in $\mathbb{Z}[Q]/(Q + 1)$ or $\mathbb{Z}[Q]/(Q^2 + Q + 1)$; an independent symbolic calculation checks these displayed identities but is not a replacement for them. □

The theorem does not say that every congruence subsequence fails to stabilize. Some stabilize to wrong values. It says that no raw subsequence is the desired common tower.

6.6. **Two sharp obstructions to a universal disk map.** For $|Q|<1$, put

$$(Q;Q)_\infty=\prod_{n\geq 1}(1-Q^n).$$

**Proposition 6.11** (Radial endpoints do not determine a disk series)**.** *For every $P(Q)\in\mathbb{C}[Q]$, every $\Delta\in\mathbb{Q}$, and every root of unity $\xi$,*

$$\mathrm{Rad}_{Q\to\xi}\, Q^{\Delta}P(Q)(Q;Q)_\infty=0$$

*on any fixed lifted branch. Hence a disk function $G$ and*

$$G(Q)+Q^{\Delta}P(Q)(Q;Q)_\infty$$

*have the same radial values at all roots whenever those values exist. Therefore the endpoint theorem cannot reconstruct $\widehat{Z}_\Gamma(Q)$ from $J_M$.*

*Proof.* The eta transformation law gives exponential decay of the infinite product along every fixed lifted radial approach. Polynomial and rational-power factors stay bounded there, so they cannot detect the added flat term. Thus radial endpoint data are compatible with many different disk functions.

Write $\xi=e^{2\pi ih/r}$, $(h,r)=1$, and $\tau=h/r+it/(2\pi)$, so $Q=e^{2\pi i\tau}$. Choose $\gamma\in\mathrm{SL}_2(\mathbb{Z})$ whose lower row is $(r,-h)$. Then

$$\mathrm{Im}(\gamma\tau)=\frac{2\pi}{r^2t}.$$

The Dedekind eta transformation law and $(Q;Q)_\infty=Q^{-1/24}\eta(\tau)$ give

$$|(Q;Q)_\infty|=O\left(t^{-1/2}\exp\left[-\frac{\pi^2}{6r^2t}\right]\right).$$

This tends to zero faster than every power of $t$. On the fixed branch, $Q^{\Delta}$ and $P(Q)$ remain bounded, proving the vanishing and its additive consequence. □

**Corollary 6.12** (No global polynomial-preserving Habiro-to-disk ring map)**.** *There is no continuous ring homomorphism*

$$\widehat{\mathbb{Z}[Q]}_{\mathrm{H}}\longrightarrow\mathbb{Z}[[Q]]$$

*from the Habiro topology to the $Q$-adic topology that restricts to the identity on $\mathbb{Z}[Q]$.*

This is the ring-map corollary of the stronger canonical companion theorem [25, Theorem 2.2], which rules out even a continuous additive map fixing the polynomial subring. The theorem compares completion topologies; it does not obstruct the separately supplied radial data in Theorem 6.5.

*Remark* 6.13 (Exact closure and remaining boundary). The radial endpoint equality is proved for negative-definite unimodular plumbing trees satisfying (6.1), in every Heegaard genus. The $\Sigma(2,3,7)$ Bailey identity gives a second exact route to the same endpoint and also proves that its raw matched-order polynomials are not a common Habiro tower. No result in this section gives a generic boundary state, a natural Habiro-to-disk homomorphism, a disk series for arbitrary three-manifolds or arbitrary plumbings, a non-IHS vector of blocks, or equality of disk series from equality of their radial endpoints.

## 7. The refined scalar vacuum and its limitations

The ordinary closed theorem leaves a narrower refined question: which scalar vacuum survives after an additional refinement parameter is introduced? This section records the corrected scalar statement and separates it from the unproved refined state-space and arbitrary-genus claims.

7.1. **The scalar refined vacuum.** Let $x$ be the multiplicative holonomy variable. Fix branches of $Q^{1/4}$ and $x^{1/2}$, equivalently a finite cover of $(\mathbb{C}^*)^2$. For each integer $\nu \geq 0$, the scalar below belongs to the following monomial multiple of the polynomial ring $\mathbb{Z}[Q,x]$:

$$Q^{-\nu(\nu+1)/4}x^{-(\nu+1)/2}\mathbb{Z}[Q,x] \subset \mathbb{Z}[Q^{\pm 1/4}, x^{\pm 1/2}]. \tag{7.1}$$

As a $Q$-disk object it is holomorphic only after removal of the displayed monomial prefactor; no regularity of the raw expression at $Q=0$ is asserted.

Use the rank-one Aganagic–Shakirov refinement parameter [1]

$$t_{\mathrm{AS}} = Q^B, \qquad B = \nu + 1,$$

so the ordinary theory is $B=1$, equivalently $\nu=0$. If the refinement variable is $u=Q^\nu$, then $t_{\mathrm{AS}} = Qu$. Equivalently, $B=\beta_{\mathrm{AS}}$ and $\nu = \beta_{\mathrm{AS}} - 1$, where $\beta_{\mathrm{AS}}$ is the exponent in the source convention $t = Q^{\beta_{\mathrm{AS}}}$. In $t_{\mathrm{AS}}$ and $\beta_{\mathrm{AS}}$, the subscript refers to Aganagic–Shakirov; the matrix superscript AS in Section 4 refers instead to Arthamonov–Shakirov. The shift by one is essential: omitting it moves the unrefined point and corrupts the cap normalization.

The refined mapping-class matrices are projective, so their diagonal twist is initially determined only up to a common nonzero scalar. Write a raw projective representative as $T_j^{\mathrm{proj}}$ and fix the vacuum normalization by

$$\widetilde{T}_j := \frac{T_j^{\mathrm{proj}}}{T_0^{\mathrm{proj}}} = Q^{-j^2/4}t_{\mathrm{AS}}^{-j/2}. \tag{7.2}$$

Only $\widetilde{T}$ is used below; no assertion that the raw projective representative has $T_0^{\mathrm{proj}} = 1$ is needed. This is the operator denoted $T$ in [3]; their positive genus-two $A$-curve twist is $T^{-1}$. Thus the negative exponents in (7.2) are a declared twist-direction convention, not an unrecorded inversion.

For $\nu \in \mathbb{Z}_{\geq 0}$, define

$$C_\nu(x;Q) = Q^{-\nu(\nu+1)/4}x^{-(\nu+1)/2}(x;Q)_{\nu+1}.$$

We write $\Delta_{Q,t}(x)$ for the rank-one refined Weyl denominator in the solid-torus wavefunction convention of [1].

**Theorem 7.1** (Scalar refined solid-torus vacuum)**.** *For every $\nu \geq 0$, with $B = \nu+1$,*

$$\boxed{C_\nu(x;Q) = \Delta_{Q,Q^B}(x) = \prod_{m=0}^{B-1}\left(Q^{-m/2}x^{-1/2} - Q^{m/2}x^{1/2}\right).}$$

*Consequently $C_\nu$, in the fixed-cover target (7.1), is the wavefunction of the scalar Macdonald vacuum state $|0\rangle$, and the vacuum-normalized refined twist acts on that state by $\widetilde{T}_0 = 1$.*

*Proof.* Factor the $m$-th term as

$$Q^{-m/2}x^{-1/2}(1-Q^m x).$$

Multiplication over $0 \leq m \leq B-1$ gives

$$Q^{-B(B-1)/4}x^{-B/2}(x;Q)_B.$$

Substituting $B = \nu+1$ gives exactly $C_\nu(x;Q)$. In the solid-torus construction of [1], the Macdonald wavefunction of the state labeled by $j$ is $\Delta_{Q,t_{\mathrm{AS}}}M_j$, where $M_j$ is the rank-one Macdonald polynomial with representation label $j$. Since $M_0 = 1$, the displayed product is the wavefunction of $|0\rangle$. Dividing the raw projective twist by its common vacuum scalar as in (7.2) gives $\widetilde{T}_0 = 1$. □

*Remark* 7.2 (Retracted support-rank inference). The $\lfloor(\nu+3)/2\rfloor$ orbits obtained by pairing opposite holonomy exponents in the Laurent expansion of $C_\nu$ do not count vacuum states. They group monomial terms in one holonomy wavefunction. The representation-label basis is the Macdonald basis, not the monomial basis. Thus the previously circulated support-rank inference that these orbits force a vector-valued vacuum, together with its asserted minimal rank, is retracted.

A refinement taking values in a vector space or an invertible coefficient module may still require additional geometric or analytic input, such as defects, a choice of polarization, or an independently constructed disk transform. The theorem only says that such an enhancement is not forced by the Laurent support of the solid-torus cap.

7.2. **A formal split coefficient object.** Put $Q = A^4$, $u = T^2$, and $\Lambda_{\mathrm{ref}} = \mathbb{Z}[A, T]$. Here $T$ is a coefficient variable, distinct from the twist operator $\widetilde{T}$ above. Define

$$\widehat{\Lambda}_{\mathrm{ref,disk}} = \varprojlim_{r} \Lambda_{\mathrm{ref}}/(A,T)^r, \qquad \widehat{\Lambda}_{\mathrm{ref,cyc}} = \varprojlim_{N} \Lambda_{\mathrm{ref}}/((Q;Q)_N).$$

Define the joint coefficient object by the product-ideal system

$$\widehat{\Lambda}_{\mathrm{ref,joint}} = \varprojlim_{r,N} \Lambda_{\mathrm{ref}}/\big((A,T)^r((Q;Q)_N)\big).$$

**Proposition 7.3** (Formal split coefficient object)**.** *There is a canonical coefficient-ring isomorphism*

$$\boxed{\widehat{\Lambda}_{\mathrm{ref,joint}} \cong \widehat{\Lambda}_{\mathrm{ref,disk}} \times \widehat{\Lambda}_{\mathrm{ref,cyc}}.}$$

*Proof.* The polynomial $(Q;Q)_N = (A^4;A^4)_N$ is congruent to one modulo $A$, hence is a unit modulo every $(A,T)^r$. Therefore the two stage ideals are comaximal. The Chinese remainder theorem gives the finite-stage product, compatibly in $r$ and $N$; passage to inverse limits gives the result. □

*Remark* 7.4 (Limits of the formal product decomposition). The displayed isomorphism is an algebraic decomposition of the stated product-ideal inverse limit. It does not make the specialization $u = Q^\nu$, with $u = T^2$, continuous on the disk factor. At the unrefined point $\nu = 0$, that specialization requires $T^2 \mapsto 1$, whereas $T^2$ is topologically nilpotent in the $(A,T)$-adic topology. Its powers therefore converge to zero while their images are all one. Consequently the map is discontinuous already at $\nu = 0$. No generic refined coefficient topology, unrefined-limit theorem, or disk/cyclotomic comparison follows from Proposition 7.3.

*Remark* 7.5 (Viability is not construction). The scalar-vacuum identity proves that a scalar refined target is not ruled out by the cap. It does not construct generic-$(Q,t)$ recoupling, refined slide descent, a refined Hopf/$S$ row, anomaly cancellation, stabilization, or an independently identified disk block.

*Remark* 7.6 (No radial shortcut). Neither exact finite-root values nor a cyclotomic refined element determine a monomial-prefactored refined disk block on a fixed cover. The disk coordinate must be constructed or identified independently; the unrefined polynomial-identity no-go remains in force after adding a refinement parameter.

The scalar identity and formal product decomposition are the complete refined output of this paper. Generic recoupling, slide descent, caps, anomaly cancellation, and arbitrary-genus coherence remain outside its scope.

## 8. Closed outputs, scope, and limitations

The paper produces four kinds of output: capped finite-root scalars, their Habiro lift, restricted radial endpoints of independently defined plumbing blocks, and the corrected scalar refinement. The Poincaré benchmark fixes the marked orientation, finite scalar, distinguished compatible lift, and exceptional endpoint; it is not a general reconstruction of disk data.

(1) On the unimodular-$C_\phi$ locus, the capped finite-root scalar uses $\mathcal{D}_p$ for the finite-level total quantum dimension, $\rho^{\mathrm{Hdg}}_{g,p}(\widetilde{\phi})$ for the Heegaard operator, and $\mathcal{A}^{\mathrm{std}}_{g,p}$ for the resulting normalized closed scalar. In particular, the letter $A$ in this scalar's name is not a skein or root parameter. Explicitly,
$$\mathcal{A}^{\mathrm{std}}_{g,p}(\phi) = \mathcal{D}_p^{g-1}\langle 0|\rho^{\mathrm{Hdg}}_{g,p}(\widetilde{\phi})|0\rangle$$
is a normalized closed invariant at every odd prime $p \geq 5$.

(2) The closed scalar descends to $J_{M_\phi} \in \widehat{\mathbb{Z}[Q]}_{\mathrm{H}}$, independent of the Heegaard genus and marking. Its polynomial truncations provide simultaneous finite-root and Ohtsuki control.

(3) If the same oriented manifold is represented by a negative-definite unimodular plumbing tree satisfying (6.1), the independently defined disk block has radial endpoint prescribed by $J_{M_\phi}$ through Theorem 6.5.

(4) In the refined rank-one calculation, the scalar vacuum is $C_\nu(x;Q) = \Delta_{Q,Q^{\nu+1}}(x)$. It fixes the shifted refinement parameter and the scalar cap normalization; it does not construct a refined modular functor.

Each output has a specific reconstruction limit. A closed scalar does not reconstruct an uncapped boundary state. A Habiro element has evaluations at roots but no canonical disk value. Radial endpoint equality does not imply equality of disk series. The product of finite-root cotests is not the continuous dual of the product of primal state spaces. Finally, the unimodular block $C_\phi$ detects the integral-homology-sphere locus but does not classify the closed manifold or determine its quantum invariant.

*Remark* 8.1 (Exact boundary of the paper). No theorem in this paper supplies any of the following:

(1) a Habiro-valued or disk-valued uncontracted state for every surface;
(2) a block vector for rational homology spheres or manifolds with positive first Betti number;
(3) a radial theorem outside the exact plumbing and leaf hypotheses of Theorem 6.3;
(4) a uniqueness principle recovering a disk series from its root endpoints;
(5) a continuous ring map from the full Habiro completion to the $Q$-adic disk completion that fixes polynomials;
(6) a refined representation, recoupling calculus, slide theorem, cap, anomaly, or stabilization theorem in arbitrary genus.

The Poincaré lift uses additional manifold-specific disk data, whereas the $\Sigma(2,3,7)$ Bailey identity has the correct endpoint but no matched-order projective tower. Habiro descent is therefore a Heegaard realization of the known unified invariant, and the radial statement is the attributed composition in Murakami's exact range. The independent boundary results are the completion/no-map, endpoint-nonuniqueness, Bailey-tower, and refined-vacuum statements.

## References

1. Mina Aganagic and Shamil Shakirov, *Knot homology and refined Chern–Simons index*, Communications in Mathematical Physics **333** (2015), no. 1, 187–228, doi:10.1007/s00220-014-2197-4; Preprint title: *Knot homology from refined Chern–Simons theory.* arXiv:1105.5117.

2. Gorjan Alagic and Catharine Lo, *Quantum invariants of 3-manifolds and NP vs. #P*, Quantum Information and Computation **17** (2017), no. 1–2, 125–146, doi:10.26421/QIC17.1-2-8; arXiv:1411.6049.
3. Semeon Arthamonov and Shamil Shakirov, *Refined Chern–Simons theory in genus two*, Journal of Knot Theory and Its Ramifications **29** (2020), no. 7, Article 2050044, doi:10.1142/S0218216520500443; arXiv:1504.02620v3.
4. Kenneth L. Baker, *The Poincaré homology sphere, lens space surgeries, and some knots with tunnel number two*, Pacific Journal of Mathematics **305** (2020), no. 1, 1–27, doi:10.2140/pjm.2020.305.1; With an appendix by Neil R. Hoffman; arXiv:1504.06682.
5. Christian Blanchet, Nathan Habegger, Gregor Masbaum, and Pierre Vogel, *Topological quantum field theories derived from the Kauffman bracket*, Topology **34** (1995), no. 4, 883–927, doi:10.1016/0040-9383(94)00051-4.
6. Miranda C. N. Cheng, Sungbong Chun, Francesca Ferrari, Sergei Gukov, and Sarah M. Harrison, *3d Modularity*, Journal of High Energy Physics **2019** (2019), no. 10, Article 010, doi:10.1007/JHEP10(2019)010; Version 2, 27 May 2020; arXiv:1809.10148v2.
7. Francesco Costantino, *Integrality of Kauffman brackets of trivalent graphs*, Quantum Topology **5** (2014), no. 2, 143–184, doi:10.4171/QT/49; arXiv:0908.0542.
8. Patrick M. Gilmer and Gregor Masbaum, *Integral lattices in TQFT*, Annales Scientifiques de l'École Normale Supérieure (4) **40** (2007), no. 5, 815–844, doi:10.1016/j.ansens.2007.07.002; arXiv:math/0411029.
9. Enore Guadagnini, Philippe Mathieu, and Frank Thuillier, *Flat connections in three-manifolds and classical Chern–Simons invariant*, Nuclear Physics B **925** (2017), 536–559, doi:10.1016/j.nuclphysb.2017.10.021; arXiv:1710.09629.
10. Sergei Gukov and Ciprian Manolescu, *A two-variable series for knot complements*, Quantum Topology **12** (2021), no. 1, 1–109, doi:10.4171/QT/145; Version 2, 29 June 2020; arXiv:1904.06057v2.
11. Sergei Gukov, Marcos Mariño, and Pavel Putrov, *Resurgence in complex Chern–Simons theory*, 2016, Preprint. Version 2, 20 October 2016; arXiv:1605.07615v2.
12. Sergei Gukov, Du Pei, Pavel Putrov, and Cumrun Vafa, *BPS spectra and 3-manifold invariants*, Journal of Knot Theory and Its Ramifications **29** (2020), no. 2, Article 2040003, doi:10.1142/S0218216520400039; arXiv:1701.06567v2.
13. Sergei Gukov, Pavel Putrov, and Cumrun Vafa, *Fivebranes and 3-manifold homology*, Journal of High Energy Physics **2017** (2017), no. 7, Article 071, doi:10.1007/JHEP07(2017)071; arXiv:1602.05302v1.
14. Kazuo Habiro, *A unified Witten–Reshetikhin–Turaev invariant for integral homology spheres*, Inventiones Mathematicae **171** (2008), no. 1, 1–81, doi:10.1007/s00222-007-0071-0; arXiv:math/0605314.
15. Søren Kold Hansen, *Reshetikhin–Turaev invariants of Seifert 3-manifolds and a rational surgery formula*, Algebraic & Geometric Topology **1** (2001), 627–686, doi:10.2140/agt.2001.1.627; arXiv:math/0111057.
16. Kazuhiro Hikami, *Mock (false) theta functions as quantum invariants*, Regular and Chaotic Dynamics **10** (2005), no. 4, 509–530, doi:10.1070/RD2005v010n04ABEH000328.
17. Rinat Kashaev and Alexis Virelizier, *Generalized Kuperberg invariants of 3-manifolds*, Algebraic & Geometric Topology **19** (2019), no. 5, 2575–2624, doi:10.2140/agt.2019.19.2575; arXiv:1805.00413.
18. Ruth Lawrence and Don Zagier, *Modular forms and quantum invariants of 3-manifolds*, Asian Journal of Mathematics **3** (1999), no. 1, 93–108, doi:10.4310/AJM.1999.v3.n1.a5.
19. Robert Lipshitz, Peter S. Ozsváth, and Dylan P. Thurston, *Computing $\widehat{HF}$ by factoring mapping classes*, Geometry & Topology **18** (2014), no. 5, 2547–2681, doi:10.2140/gt.2014.18.2547; Version 4, 9 February 2015; arXiv:1010.2550v4.
20. Jeremy Lovejoy, Robert Osburn, and Matthias Storzer, *Bailey pairs, Eichler integrals and unified Witten–Reshetikhin–Turaev invariants*, 2026, Preprint. arXiv:2605.15740.
21. Yuya Murakami, *A proof of a conjecture of Gukov–Pei–Putrov–Vafa*, Communications in Mathematical Physics **405** (2024), no. 11, Article 274, doi:10.1007/s00220-024-05136-x; Version 3, 3 September 2024; arXiv:2302.13526v3.
22. ———, *Witten–Reshetikhin–Turaev invariants and homological blocks for plumbed homology spheres*, Communications in Number Theory and Physics **18** (2024), no. 2, 371–403, doi:10.4310/CNTP.2024.v18.n2.a3; Version 2, 4 April 2024; arXiv:2205.01282v2.
23. Olga Plamenevskaya, *A combinatorial description of the Heegaard Floer contact invariant*, Algebraic & Geometric Topology **7** (2007), no. 3, 1201–1209, doi:10.2140/agt.2007.7.1201; arXiv:math/0612322.
24. Hao-Yu Sun, *Integral root fibers and closed factorizations: Pairing maps, Rees covariance, caps, and sewing*, Hexagon preprint, 2026, hexagon:2610.00340v1.
25. ———, *Marked Heegaard boundary modules: Filling, joint completion, and integral lattices*, Hexagon preprint, 2026, hexagon:2610.00339v1.


Weinberg Institute, The University of Texas at Austin, 2515 Speedway, C1600, Austin, Texas 78712, USA

SpaceX, USA
*Email address*: hkdavidsun@utexas.edu